



# Three decades of accomplishments in computational fluid dynamics

J.S. Shang\*

*Department of Mechanical and Materials Science, Wright State University, Dayton, OH 45435-0001, USA*

## Abstract

A glance back on significant accomplishments in computational fluid dynamics for aerodynamic application has been performed to highlight the outstanding achievements by pioneers of this discipline. It is an ardent hope that this abridged literature review will aid to reaffirm excellence in research and to identify knowledge shortfalls both in fluid dynamics and its modeling and simulation capability. The future modeling and simulation technology needs, as well as potential and fertile research areas are offered for consideration.

© 2004 Elsevier Ltd. All rights reserved.

## Contents

1. Historical perspective . . . . .	174
2. Governing equations . . . . .	176
3. Early milestones . . . . .	177
4. Achievements in the eighties . . . . .	180
4.1. Finite-volume methods . . . . .	180
4.2. Characteristic-based methods . . . . .	181
4.3. Unstructured grid technique . . . . .	182
5. Recent progress . . . . .	184
5.1. High-resolution algorithms . . . . .	184
5.2. DNS and LES . . . . .	185
6. Interdisciplinary computing simulation . . . . .	187
6.1. Aeroelasticity . . . . .	187
6.2. Aerothermodynamics . . . . .	188
6.3. Computational electromagnetics . . . . .	190
6.4. Computational magneto-fluid dynamics . . . . .	191
7. Outlook . . . . .	193
8. Epilogue . . . . .	194
Acknowledgements . . . . .	194
References . . . . .	194

\*Tel.: +1-937-775-5094; fax: +1-937-775-5009.  
E-mail address: [jshang@cs.wright.edu](mailto:jshang@cs.wright.edu) (J.S. Shang).

Nomenclature			
$A$	elementary area of control surface	$\kappa$	heat conductivity
$B$	magnetic flux density	$\lambda$	bulk viscosity
$E$	electric field intensity	$\mu$	molecular viscosity
$F$	flux vector	$\rho$	density
$J$	electric current density	$\tau$	shear stress
$n$	surface outward normal	<i>Superscripts</i>	
$U$	dependent variables	'	denotes fluctuating property
$V$	elementary control volume	–	denotes vector
$Q$	radiant heat flux	=	denotes tensor

## 1. Historical perspective

The development of computational fluid dynamics (CFD) can be traced back as far as the early 1900s. The pioneering efforts by Richardson [1], Courant, Friedrichs, and Lewy [2], Southwell [3], von Neumann [4], Lax [5], as well as Godunov [6] address the fundamental issues in numerical analyses for CFD. It is immediately clear that a major portion of these efforts was focused on one of the most difficult problems in resolving the discontinuous fluid phenomena in a discrete space—the Riemann problem [7]. As it will be seen later, it remains the most studied problem in CFD. However, if one is interested in viscous flow simulation, Thom [8] probably obtained the first-ever numerical solution by solving the partial differential equation for a low speed flow past a circular cylinder. For a scholarly description of the CFD historical perspective, the books by Roache [9] and Tannehill, Anderson, and Pletcher [10] are highly recommended.

In the early 1940s, finite-difference methods for solving partial differential equations were put to use in practical problems at Los Alamos National Laboratory with the first electronic computer. These works were strictly limited to atomic weapon system development and wartime technology. The applications widened to include fluid dynamics when the ENIAC was installed at Aberdeen. The advent of the computer has revolutionized a wide range of scientific research; however, fluid dynamics is the most affected by this revolution. The computational physicist can now add insight and independent views to hasten the maturation of the previously unsolvable nonlinear problems. At the very beginning, the approach of CFD is to solve the governing equations in discrete space with uncompromising rigor. By imposing the proper initial and boundary conditions and without ad hoc simplifying approximations, the computing simulation is an imitation of a physical experiment.

Harlow first proposed the celebrated particle-in-cell (PIC) method in 1957 at Los Alamos National Laboratory [11]. This method uses a combination

Lagrangian–Eulerian description of the fluid motion. In discrete space, the solving procedure consists of fixed Eulerian cells through which the fluid moves. The fluid is represented by Lagrangian mass particles with a fixed mass of fluid. The sum of the particle masses within the cell is the mass of the cell. The calculation proceeds through a sequence of finite time steps. After the particle transport is completed, final values of internal energy and velocity are obtained from the new total mass, momentum, and energy in the cells. The sum of these final values of the system is then checked for conservation before advancing to the next time level. In short, the PIC method has demonstrated to be well suited to study the time dependent and multi-dimensional fluid motion. The effectiveness of this method is demonstrated through the applications to shock interaction by Evans et al., supersonic wakes by Amsden and Harlow, as well as to hypersonic sharp leading edge flows by Butler [12–14].

The development of this numerical procedure was accompanied by exhaustive proof in order to illustrate the range of validity of the approximations. The PIC method actually set the standards for the future development of all CFD algorithms and numerical procedures. The detailed derivation of all pertinent formulations and extensive discussions on computational accuracy and limits of applicability become the accepted tradition in CFD research. At that time, the computed resource was severely limited and allowed only a small number of representative calculations in an investigation; and yet the experience has shown that the extensive and detailed information obtainable from CFD is immeasurable. The complementary contribution to better understand the basic physics with experiments and theoretical analysis is fully appreciated.

A fluid dynamic problem of great concern for aerodynamic performance is that of flow separation at which point the boundary-layer approximation breaks down. Lees and his students [15] led the first few well-known applications for complex aerodynamic problems involving boundary-layer/shock-wave interaction. His basic approach is built on the integral momentum

equation and his incisive insight on the self-similar boundary layer. The interacting boundary solution method eventually adopted the boundary-layer code developed by a CFD pioneer, Davis [16]. Davis actually solved the multi-dimensional compressible boundary-layer equation based on the physics by a combined implicit–explicit, finite-difference approximation. He solved the rapidly changing and steep flow field gradient across the boundary layer by the tridiagonal Thomas algorithm, and the relatively slow varying streamwise variation by a forward differencing scheme. His numerical procedure for solving the compressible boundary-layer equation is accurate and robust.

The separated flow solution was recoverable by a trial-and-error method; the final solution is the numerical result that passed the saddle point at flow separation. In this connection, the triple deck theory of Stewartson [17] has provided a scaling law for the interacting boundary layers and demonstrated that the singular point of flow separation in the interacting boundary layer is indeed removable. This scaling law was successfully incorporated into the interacting laminar boundary-layer method to provide insight into the evolution of the separating flow structure [18].

For inviscid flow in the supersonic domain, the method of characteristics has been developed to a very high level of sophistication for three-dimensional flows. In fact, Rakich [19], another pioneer of CFD, devised a complex three-dimensional network of grid points to describe the intersections of the Mach cone and stream surface. The bicharacteristics that describe the compatibility conditions are partial differential equations containing cross-derivatives normal to the characteristics. For steady supersonic blunt body simulation, a set of initial data is needed for the hyperbolic equation system. These initial values, downstream of the limiting characteristics, may not be available for complex aerodynamic shapes, thus limiting its applications. However, this limitation was removed by the work of Moretti and Abbett [20]. They solved the time-dependent Euler equation by a finite-difference method, and the flow field was obtained as the steady-state asymptote. Their work has made two very important contributions to CFD; first, the time marching formulation permits the unsteady Euler equation retaining the hyperbolic formulation even for the subsonic flows. Second, they demonstrate that the Rankine–Hugoniot shock jump condition can be captured by the finite-difference approximation. Meanwhile, the vortex lattice method derived from the small perturbation theory was advanced to application for inviscid subsonic flows over aircraft [21]. This simple yet elegant method is still in use for commercial aircraft design and becomes a classic example in engineering that followed the axiom that was frequently attributed to Einstein, “keep it simple but not simpler”.

The first coherent and structured CFD organization solely for aerodynamic application was the brainchild of Dean Chapman, then the Director of Aeronautical Science Directorate of the NASA Ames Research Center. He successfully recruited and nurtured a large group of devoted talent for CFD. During that time, a rare genius in digital computer design, Seymour Cray made high-speed computers commercially available such as CDC6400 and CDC 7600. The combination of talent and support infrastructure led to a revolutionary advance in computational aerodynamic research. It was an unprecedented, and still never duplicated, amount of attention to detail and encouragement by organization leaders at the national level to a technical endeavor. For example, any CFD presentation from the Ames Research Center to a professional society was reviewed and rehearsed by the then Center Director, Hans Mark. It remains a shining case study of how to develop cutting edge technology in any arena. The research leadership role was entrusted on the shoulders of Harvard Lomax and Robert MacCormack. They carried out their duty faithfully and exerted their effort to achieve a new culture for scientific excellence. Therefore, it should not be surprising that a large group of legendary scientists were trained and got their baptism in CFD. The group of luminaries includes William Ballhaus, Richard Beam, Steven Diewert, C.M. Hung, John Kim, Paul Kutler, Parviz Moin, Earl Murman, Thomas Pulliam, Joseph Steger, Robert Warming, Helen Yee, and many others. The impact of the Ames Research Center to the CFD community extends worldwide; distinguished scientists such as Kozo Fujii and S. Obayashi of Japan, Rizzi of Sweden, as well as Wolfgang Schmidt of Germany have either an extensive visiting tour or sustained collaboration with scientists at the NASA Ames Research Center.

Equally important, the Ames Research Center has not only set the standard for scientific research, but also established the collaborative culture in the CFD community. The close working relationship among researchers at the center and a large group of constantly circulating visiting scientists through the center actually created a close-knit CFD community. A tradition of hard working, generously sharing, and strong mutual support was achieved and maintained in a very competitive environment. One cannot help but remember the long working hours, the endless toiling, but exciting challenge for gaining new knowledge, and the wonderful times together with respected colleagues. This goodwill and unwritten mutual esteem have been sustained and are apparent in all international symposia, even today.

The successful activities at the NASA Ames Research Center inspires similar activity at other NASA science and technology centers such as the Langley and now Glenn Centers. The military service branches also

appreciated the need to develop this modeling and simulation technology. CFD research groups were also organized in the Air Force Research Laboratory, Army Research Laboratory, and Navy Research Laboratory. In order to gain a global competitive edge, CFD research also thrived in the aerospace industries. Boeing, General Dynamics, Lockheed, McDonnell, Douglas, Northrop, and Grumman aircraft companies also established sizable research and development CFD teams. At the beginning of CFD development the flow of knowledge was highly nontraditional. In a stark contrast to most scientific discipline development, the traditional path of knowledge flow from academia to government and industry was reversed. One cannot help but believe this was the beginning of 30 years of galloping of CFD research.

## 2. Governing equations

The genesis of CFD has evolved in solving the time-dependent Navier–Stokes equations, a system of five nonlinear partial differential equations for three-dimensional fluid motion. This set of governing equations for incompressible flow has been known since 1827 [22]. It becomes conventional to refer to the complete set of equations of fluid motion as the Navier–Stokes equations for compressible medium including Fourier’s law for conducting heat transfer. The Navier–Stokes equations are the macroscopic description of the conservation laws of mass, momentum, and energy. In the Eulerian frame of reference, these conservation laws in integral form are

$$\frac{\partial}{\partial t} \int \int \int \rho \, dV + \int \int \bar{n} \cdot \rho \bar{u} \, dA = 0, \quad (1)$$

$$\begin{aligned} \frac{\partial}{\partial t} \int \int \int \rho \bar{u} \, dV + \int \int \bar{n} \cdot \rho \bar{u} \bar{u} \, dA \\ = \int \int \bar{n} \cdot \bar{\tau} \, dA + \int \int \int \rho \bar{f} \, dV, \end{aligned} \quad (2)$$

$$\begin{aligned} \frac{\partial}{\partial t} \int \int \int \rho e \, dV + \int \int \bar{n} \cdot \rho e \bar{u} \, dA \\ = \int \int \bar{n} \cdot (\bar{u} \cdot \bar{\tau} - \bar{q}) \, dA + \int \int \int \rho (\bar{f} \cdot \bar{u} + Q) \, dV. \end{aligned} \quad (3)$$

The integral equations hold for any control volume element contained in the flow field and are the foundation for the conservation law and finite-volume algorithm. The equivalent differential equations are obtained by a limiting process of the control volume. Through Gauss’ divergence theorem, the governing equations become

$$\frac{\partial \rho}{\partial t} + \nabla \cdot \rho \bar{u} = 0, \quad (4)$$

$$\frac{\partial \rho \bar{u}}{\partial t} + \nabla \cdot (\rho \bar{u} \bar{u} - \bar{\tau}) - \rho \bar{f} = 0, \quad (5)$$

$$\frac{\partial \rho e}{\partial t} + \nabla \cdot (\rho e \bar{u} - \bar{u} \cdot \bar{\tau} + \bar{q}) - \rho (\bar{f} \cdot \bar{u} + Q) = 0. \quad (6)$$

In these equations, the shear stress includes the Reynolds stress tensor and the heat transfer contains Fourier’s law for heat conduction, as well as the energy transfer by turbulent fluctuations.  $Q$  is the heat sink or source within the control volume, i.e. the radiation heat transfers, and  $\bar{f}$  is the external force exerted on the gas medium.

$$\bar{\tau} = (-p + \lambda \nabla \cdot \bar{u}) \bar{I} + \mu (\nabla + \nabla') \bar{u} - \overline{\rho u' u'},$$

$$\bar{q} = -\kappa \nabla T + \overline{\rho e' u'}.$$

The Navier–Stokes equations in this form are classified as the incompletely parabolic differential system [23]. The equation system is not closed: there are five equations but nine dependent variables ( $u, v, w, \rho, p, T, \mu, \lambda,$  and  $\kappa$ ). Additional equations must be introduced through the constitutive relations for the transport properties of the fluid medium and the equation of state.

For laminar flow, with a set of appropriate initial and boundary conditions, the differential equation system is solvable in principle. For turbulent flow, the current computational capability is unable to resolve the fluid motion in the Kolmogorov microscales [24]. One must be satisfied with the solution of the ensemble average with turbulence closure models. The ensemble average process is equivalent to the time average for statistically stationary flow. However, this process also eliminates several key characteristics of turbulence—the frequency, phase, and wavelength of the fluctuating motion. This is usually not critical for some practical applications, but remains as the Achilles’ heel of CFD. To date the most widely used ensemble average is mass–weight, due to Favre [25], and is based on the fact that the average mass of fluid in a control volume moves at a constant mean mass–weight velocity. This observation is also supported by the fact that the density variation has a volumetric, rather than a dynamic effect on the velocity field in a compressible turbulent flow.

In literature, the mass–average Navier–Stokes equations are written in flux vector form. The Cartesian coordinates are always adopted as the basic frame of reference for all successive coordinate transformations necessary to describe a specific configuration. The flux vectors are often split into the inviscid and viscous components subject to different numerical approximations.

$$\frac{\partial U}{\partial t} + \frac{\partial F_x}{\partial x} + \frac{\partial F_y}{\partial y} + \frac{\partial F_z}{\partial z} = 0, \quad (7)$$

where the dependent variables and the flux vector components in three spatial dimensions are

$$U = [\rho, \rho u, \rho v, \rho w, \rho e]^{-T}$$

$$F_x = \begin{bmatrix} \rho u \\ \rho u^2 + p - \tau_{xx} \\ \rho u v - \tau_{xy} \\ \rho u w - \tau_{xz} \\ (\rho e + p)u - (u\tau_{xx} + v\tau_{xy} + w\tau_{xz}) + q_x \end{bmatrix},$$

$$F_y = \begin{bmatrix} \rho v \\ \rho u v - \tau_{xy} \\ \rho v^2 + p - \tau_{yy} \\ \rho v w - \tau_{yz} \\ (\rho e + p)v - (u\tau_{xy} + v\tau_{yy} + w\tau_{yz}) + q_y \end{bmatrix},$$

$$F_z = \begin{bmatrix} \rho w \\ \rho u w - \tau_{xz} \\ \rho v w - \tau_{yz} \\ \rho w^2 + p - \tau_{zz} \\ (\rho e + p)w - (u\tau_{xz} + v\tau_{yz} + w\tau_{zz}) + q_z \end{bmatrix}.$$

In practical applications via a finite-difference method, the flux vector equations are always transformed into a generalized curvilinear, body-oriented coordinate system to facility the boundary conditions implementation. By invoking a metrics identity from coordinate transformation, the flux vector from of the Navier–Stokes equations for a finite-difference approximation can still retain the strong conservation form. Now the flux vector components explicitly contain the Jacobian of coordinate transformation,  $J$ .

$$\frac{\partial U}{\partial t} + \frac{\partial F_\xi}{\partial \xi} + \frac{\partial F_\eta}{\partial \eta} + \frac{\partial F_\zeta}{\partial \zeta} = 0, \tag{8}$$

$$\xi = \xi(x, y, z), \quad \eta = \eta(x, y, z), \quad \zeta = \zeta(x, y, z),$$

$$\bar{U} = \bar{U}(\rho/J, \rho u/J, \rho v/J, \rho w/J, \rho e/J).$$

The flux vectors in the transformed space become

$$F_\xi = (\xi_x F_x + \xi_y F_y + \xi_z F_z)/J,$$

$$F_\eta = (\eta_x F_x + \eta_y F_y + \eta_z F_z)/J,$$

$$F_\zeta = (\zeta_x F_x + \zeta_y F_y + \zeta_z F_z)/J.$$

Physically meaningful boundary conditions, in general, require the no-slip condition for the velocity components on the solid surface, and the prescribed surface or adiabatic condition for the temperature. The density is determined by the vanishing outward normal pressure gradient at the solid surface. This widely used numerical boundary condition is an outgrowth of the boundary-layer approximation and is further reinforced by the inner layer structure of the triple deck theory of Stewartson [17].

### 3. Early milestones

In 1969, MacCormack [26] published his first of many landmark numerical algorithm research results in the form of an explicit, predictor–corrector procedure that bears his name. His second-order accurate algorithm is known for its simplicity in programming and robustness in resolving aerodynamic problems involving extremely strong flow field gradients. A key element of this method is the often misquoted or wrongly attributed spectral damping terms built into his numerical procedure together with Baldwin [27]. This numerical damping term controls the numerical instability by adding artificial viscosity proportional to the local pressure gradient and spectral radius for shock capturing  $(|u| + c) |\nabla p|$ . The introduced truncation error is proportional to  $\Delta t (\Delta x)^3$ , which is two orders of magnitude smaller than the discrete approximation and reveals the remarkable insight of this modest scientist. The MacCormack explicit scheme has widely been used for more than 30 years as the critical research tool in CFD. Perhaps it is not surprising that this method is still in use for complex and difficult interdisciplinary investigations in penetration mechanics and electromagnetic energy deposition for aerodynamic control. For this reason, this fundamental numerical algorithm is still taught in most CFD classes.

MacCormack’s lasting contribution to CFD is also reflected strongly in shock-boundary interaction problems. The physics of viscous–inviscid flow interaction must be recovered from solving the Navier–Stokes equations. The early works in compression ramp and shock-boundary interactions by Hung and MacCormack [28], Horstman et al. [29], and Shang and Hankey [30] have provided a better basic understanding of the boundary-layer separation and exposed the weakness of rudimentary turbulent closure models. The very few early solutions by solving the Reynolds-averaged Navier–Stokes equations were for shock-boundary-layer interaction over a two-dimensional compression ramp including flow separation. The comparison of the numerical simulation and a Schlieren photograph is depicted in Fig. 1 to show that the numerical results indeed capture the essential feature of this fundamental aerodynamic phenomenon. In this connection, Knight [31] also first applied this numerical technique to simulate realistic high-speed inlets for analyzing the performance of air-breathing engines. A sustained research effort in shock-boundary interactions has been maintained for the past 30 years, and recently David Dolling has summarized all these efforts in an excellent review article [32].

In the 1970s, even a three-dimensional hypersonic compression corner problem was successfully simulated using the MacCormack explicit method [33]. The computational domain of a strong hypersonic



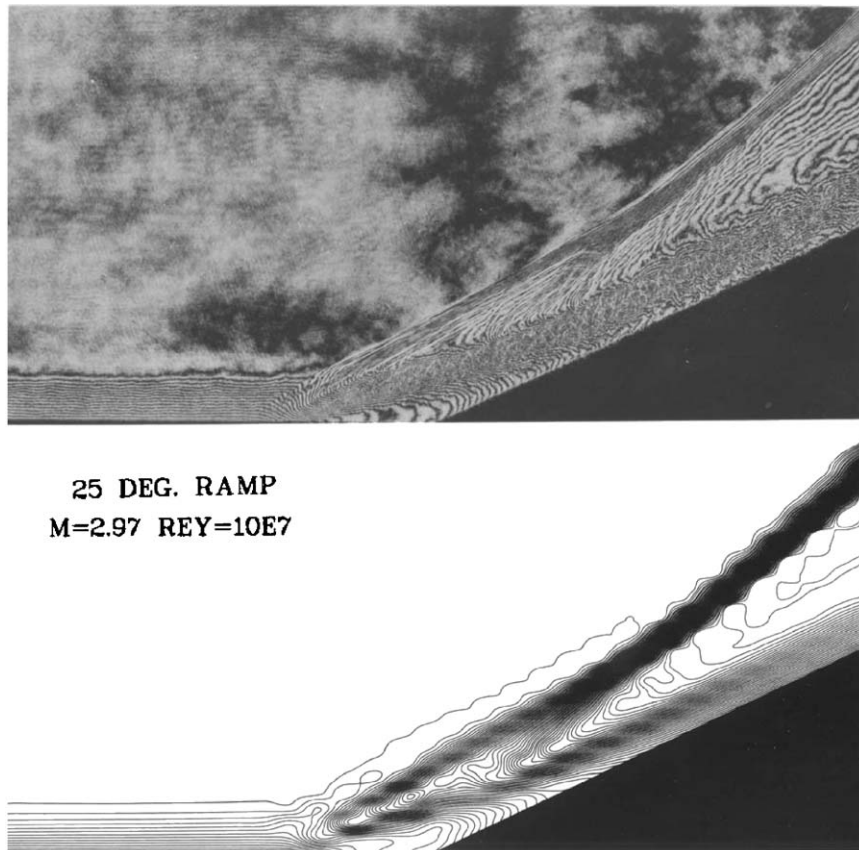


Fig. 1. Shock-boundary-layer interaction over a compression ramp.

shock-boundary-layer interaction was confined in a frustum of a rectangular pyramid by a mesh system of  $(8 \times 32 \times 36)$  bounded by a wedge and a flat plate. The mesh system consisted of a measly 9216 points, but it already occupied the complete memory capacity of the CDC 7600 computer. A physically meaningful solution was obtained by invoking the salient feature from the hypersonic equivalence principle—the dominant flow perturbation occurs mostly in the cross flow plane. The numerical results reached impressive agreement with experimental measurements in heat transfer rate and surface pressure distribution. Equally important, the triple-point shock structure was captured at the intersection of the wedge shock and the induced shock from the sharp leading edge flat plate (Fig. 2). From this calculation, the hot spot of the corner was also identified as the penetrating inviscid stream at the shock triple point. Although these types of numerical computations resolved only the essential feature of interacting flow field, it began to become a powerful tool in aerodynamic research.

Another previously unsolvable nonlinear transonic flow phenomenon has also attracted a lot of research efforts. The basic physics of transonic flow emerges from

the fact that a flow disturbance must propagate in drastically changing domains of dependence. If one opts to study transonic flow using the Euler equations, the governing nonlinear partial equations system changes from the elliptic, parabolic, and hyperbolic type corresponding to whether the flow field exists in the subsonic, transonic, or supersonic flow regimes respectively. Aside from the unknown and uncertain well-posed boundary condition criterion for the discrete approximation, there is ambiguity as how to best satisfy the directional signal propagation according to the eigenvalue of the differential system.

A breakthrough in transonic flow simulation is attributed to Murman and Cole [34]. Their novel approach was the first to use a combination of central and windward difference approximations to satisfy the domain of dependence. The transonic small disturbance theory was used to solve the flow past thin airfoils with imbedded shock waves. The governing equation is a mixed elliptic–hyperbolic differential equation that was solved by a separate difference formula in the elliptic and hyperbolic regions to account properly for the local domain of dependence. Their accomplishment again reinforces the fundamental rule in algorithm

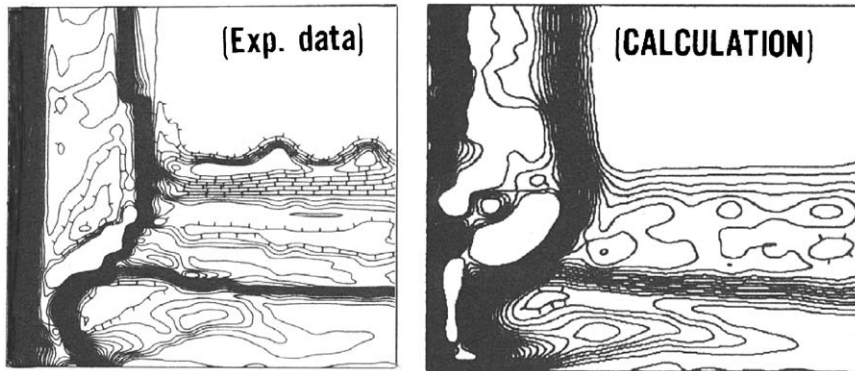


Fig. 2. Triple shock structure in a 3D corner,  $M=12.6$ .

development—the most accurate and efficient numerical procedure for problem solving is the one that best mimics the physics.

During the same time frame, Jameson [35] started to develop a widely used explicit numerical procedure for transonic flows and initiated an illuminative career and became one of the most respected leaders in CFD. The most remarkable achievements by Jameson are his emulation of the shockless transonic wing, multigrid algorithm development, and his ingenious aerodynamic optimizing techniques. His numerous contributions to transonic airfoil and wing designs have no peer and equally impressive is his natural ability in nurturing young talents and bringing out the most creativity from them.

The venturing of CFD into practical applications was greatly aided by the body orientated coordinate generation technique introduced by Thompson [36]. He ranks among all pioneers in CFD and uniquely possesses an unfailing courtesy of southern gentry. His work indeed has opened a new avenue for CFD applications to practical and complex configurations ahead of any other physics-based simulation discipline such as computational electromagnetics (CEM). For structured grid computations, the grid generation by solving partial elliptic [36], hyperbolic [37], and algebraic [38] equations is the cornerstone for application to complex configurations.

Since a major portion of engineering applications is time dependent, some numerical simulations with bodies of relative motion have to be obtained from a moving grid. When the governing equations are mapped onto a moving computational domain and solved by a finite-difference technique in the strong conservation form, the geometrical conservation law by Thomas and Lombard [39] must be observed to eliminate computational errors. In essence, the geometrical conservation law stresses the coupling between the numerical algorithms and the moving grid metric calculations.

This requirement arises from a mathematical identity in the metrics evaluation and must be satisfied simultaneously with the governing equation. The geometrical conservation law has provided a solid foundation for extending CFD applications to the moving frame of reference.

As the complexity of CFD simulations has increased, efforts were focused on accelerating the numerical convergence rate and stability of the numerical algorithm to reduce the required computing resources. It has been known for quite a while, that the implicit schemes, in general, possess the more favorable stability property for solving linear partial differential equations [40,41]. This class of algorithms is commonly referred to as the ADI (alternating direction implicit) scheme, and indeed it is unconditionally stable when applied to three-dimensional parabolic and elliptic partial differential equations and two-dimensional hyperbolic systems. Since the discrete system of equations must be solved simultaneously, a matrix inversion procedure is required. The inversion process not only needs a much greater computer addressable memory, but also may incur round-off error. However, the gain in computing stability has frequently compensated for the additional resources required over that of explicit schemes. The pioneering contributions by Briley and McDonald who used the ADI scheme to solve the Navier–Stokes equations were first published in 1970 in a laboratory report and a year later in more accessible sources in 1971 and 1974 [42,43]. Beam and Warming made sustained and substantial contributions to the factorized implicit numerical algorithms. They first presented their work in solving the compressible Navier–Stokes equations in 1977 and published it a year later [44]. This algorithm has been subjected to systematic development by an exceptional group of individuals, such as Pulliam, Steger among others, to become the most widely used numerical procedure in the CFD community for the next few decades [45].

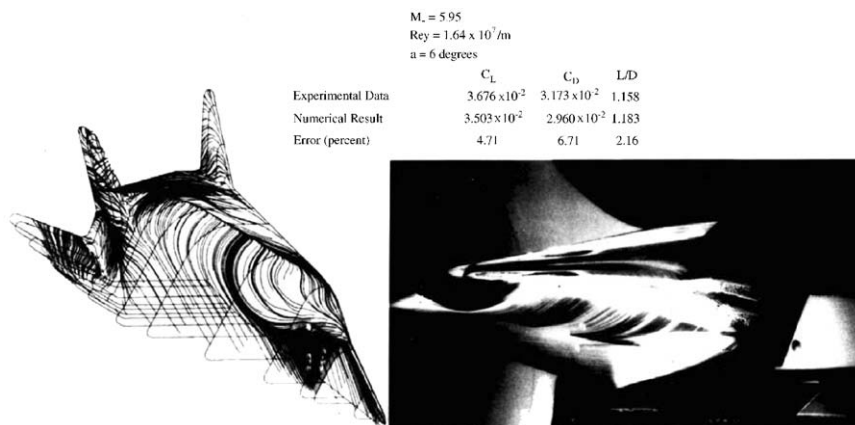


Fig. 3. Reentry vehicle X-24C-10D simulations.

An insignificant event in research that reflects the ingrained tradition of peer review and the open debate amongst the CFD community is probably worth sharing. At the AIAA 1977 Summer Meeting in Albuquerque, Briley, Warming, Lomax, and Shang got together for a technical exchange on the development and relative merits of ADI schemes. One cannot help but feel proud about the open and earnest discussion and the sense of fairness in the CFD discipline. This feeling prevailed and in 2001, when McDonald became the Director of the NASA Ames Research Center, he bestowed the coveted J. Allen Award to Dick Beam and Bob Warming for their accomplishments in developing the factored implicit numerical procedures.

The search for high computing efficiency reflects an impressive creativity in the CFD community. The Newton quadrature scheme probably has the fastest convergence rate known to us, but the scheme also requires that an initial estimate of the solution must be within a convergence tolerance. The overall convergence rate of an equation system is closely tied to the spectral radius of its eigenvalues and the elimination of error residue from its initial estimate. To achieve a fast convergence rate of an iterative approach to a steady-state asymptote for the Navier–Stokes equations, a new strategy is required. Brandt met this need by introducing the multi-grid method [46]. The basic idea is to filter out the low-frequency numerical error by interpolating the finer grid result to a coarser grid, and to obtain the correction to the fine grid by an up-sweeping process. This method has exhibited a substantial improvement of rate of iterative convergence. The attraction of the multi-grid iterative technique also lies in its broad range of applicability to CFD problems.

The introduction of the implicit and iterative algorithm, grid generation techniques, and physically based

approximations such as the parabolized [47] and thin-layer [45] Navier–Stokes equations greatly enhanced the range of CFD applications. Some early CFD applications in aerodynamics include the transonic airfoil by Levy [48], aileron buzz by Steger and Bailey [49], airfoil dynamic stall by Tassa and Sankar [50], scramjet flow field by Drummer and Weidner [51], boundary-layer instability by Fasel [52], bodies at high angle of attack by Helliwell et al. [53]. Shang and Scherr in 1985 eventually simulated the aerodynamic performance of a complete reentry vehicle (X-24C) on the Cray 1 computer using the MacCormack explicit scheme on the grid generated by Steger's hyperbolic grid generator [54]. The computed surface shear stress map and oil film pattern on a scaled X24C model is depicted in Fig. 3.

#### 4. Achievements in the eighties

##### 4.1. Finite-volume methods

The finite-volume formulation of the macroscopic conservation law is intrinsic in the Eulerian frame of reference. The concept of conservation laws is actually defined for an arbitrary control volume. The variation of dependent variables within the control volume, whether they are mass or components of momentum or internal energy, are balanced by the flux across the control surface of this volume. The basic formulation uses the integral form of the Navier–Stokes equations. The finite-volume formulation rigorously enforces the conservative law both on each elementary cell and for the complete control volume of the flow field. This formulation is less susceptible to singular behavior of a geometrical shape than the metrics of coordinate transformation in the finite-difference approximation. The first numerical



result of this formulation for the Navier–Stokes equations is attributed to MacCormack and Paullay [55], but Rizzi and Inouye first coined the term [56] finite-volume method. However, the finite-volume method was not widely used until the 1980s. Thomas and Walters [57] and MacCormack [58] implemented this formulation for the Navier–Stokes equations by an implicit Gauss-Seidel relaxation algorithm, which led to a group of robust numerical procedures as the mainstay of present CFD applications.

The basic formulation of the finite-volume scheme requires the reconstruction of the flux vector normal to the elementary volume; it is therefore natural to introduce the windward differencing approximation that had been consistently advocated by van Leer [59]. Furthermore, the reconstruction process on the control surfaces also easily permits the development of high-resolution procedures. The seminal contribution by Harten [60] for the high-order reconstruction process, and the contributions to windward approximation and total variation diminishing (TVD) scheme, and the contribution to the monotone scheme by Osher and Chakravarthy [61] should be noted.

#### 4.2. Characteristic-based methods

Using the compatibility condition to solve the steady, supersonic Euler equations was at the very beginning of aerodynamic research [5,6]. In fact, it was the genesis of the method of characteristics since 1929 by Busemann [62], and was developed further to include rotational flow by Ferri in the late 1940s [63]. However, predicting a multi-dimensional flow field that contains shock waves and contact surfaces was presented in a landmark paper by Godunov [6]. He treated discontinuities of the hyperbolic differential systems by assuming a piecewise continuous data distribution within a control volume and by solving the Riemann problem across each cell interface. The flux vector is computed by the windward approximation to satisfy the governing equation in an integral conservation form. By solving sets of Riemann problems over the entire computational domain, this approach honors the physics of domain of dependence using the correct database according to the directional propagation of wave motions.

In 1973, Boris and Book introduced the flux correction approach [64], and independently a few years later, Steger and Warming [65] introduced the flux-splitting method to the CFD community. In this outstanding work of Steger and Warming, they have shown systematically the relationship of the real eigenvalue and diagonalizable eigenvector and the split flux formulation. They have also pointed out that if the equation of state can describe the pressure as the product of density and a function of internal energy,  $P = \rho f(e)$ , the Euler equations possess the homogeneous function of

degree one property;  $\partial F / \partial x = (\partial F / \partial U)(\partial U / \partial x)$ . These properties of flux vectors together with the diagonalizable Jacobian matrices  $\partial F / \partial U$  make the split flux possible. They also pointed out that the splitting of the flux vector according to the sign of the associated eigenvalues is not unique. The flux-splitting scheme has proved to be effective in resolving the shock, but a deficiency also appears at the sonic and stagnation points. The basic issue is that the split flux components are not continuously differentiable at these points. This behavior is also the peculiarity of the approximate governing equations. van Leer addressed this shortcoming by introducing the flux difference splitting method [66]. Other ideas for splitting the Euler equations have also been introduced [10].

The basic idea of flux splitting is to process data according to the direction of information propagation and to better approximate the Riemann problem. For Navier–Stokes equations, the inviscid terms in the flux vector  $F_x, F_y,$  and  $F_z,$  Eq. (7), are the Euler equations that constitute a hyperbolic differential system with all real eigenvalues. Therefore the inviscid flux vector can be split according to the signs of their corresponding eigenvalues [65,66]. For an approximate solution in discrete space, the flux vectors are computed as a point value or values on contiguous sides of control surface. This approach for solving hyperbolic partial differential equations not only ensures the well-posed condition of the differential system, but also enhances the stability of the numerical procedure. The split fluxes of this initial-value problem are calculated by a windward algorithm to honor the zone of dependence. The splitting formulation however is only achievable for each single time–space dimension, and has an identically cyclic structure in all other spatial dimensions. The eigenvalues of the Jacobian (coefficient) matrix in  $x$ – $t$  plane are

$$\begin{aligned} \lambda_1 &= \lambda_2 = \lambda_3 = k_1 u + k_2 v + k_3 w, \\ \lambda_4 &= \lambda_1 + c(k \cdot k)^{1/2}, \\ \lambda_5 &= \lambda_1 - c(k \cdot k)^{1/2}, \end{aligned} \tag{9}$$

where  $c$  is the local speed of sound and  $k$  ( $k_1, k_2, k_3$ ) are arbitrary real numbers. According to Steger and Warming, the three-dimensional, generalized flux vector can be given as [65]

$$F = \rho / 2\gamma \times \begin{bmatrix} 2(\gamma - 1)\lambda_1 + \lambda_4 + \lambda_5 \\ 2(\gamma - 1)u\lambda_1 + (u + ck_1)\lambda_4 + (u - ck_1)\lambda_5 \\ 2(\gamma - 1)v\lambda_1 + (v + ck_2)\lambda_4 + (v - ck_2)\lambda_5 \\ 2(\gamma - 1)w\lambda_1 + (w + ck_3)\lambda_4 + (w - ck_3)\lambda_5 \\ (\gamma - 1)U^2\lambda_1 + U^+\lambda_4/2 + U^-\lambda_5/2 + W + P \end{bmatrix}, \tag{10}$$

where

$$\begin{aligned} U^2 &= u^2 + v^2 + w^2, \\ U^+ &= (u + ck_1)^2 + (v + ck_2)^2 + (w + ck_3)^2, \\ U^- &= (u - ck_1)^2 + (v - ck_2)^2 + (w - ck_3)^2, \\ W &= (3 - \gamma)(\lambda_4 + \lambda_5)c^2/2(\gamma - 1), \\ P &= 2\rho(\gamma - 1)k_1(k_2w - k_3v)\lambda_1. \end{aligned}$$

The similarity transformation  $S$ , of the Jacobian matrix  $(\partial F/\partial x)$  for the flux vector is constructed by using the eigenvectors as the column arrays. Even though the eigenvalues of the matrix contain multiplicities, the linearly independent eigenvector still can be found by reducing the coefficient matrix to the Jordan normal form. The similarity transformation exists, all flux vectors are split according to the signs of the eigenvalues to appear as

$$\begin{aligned} F^+ &= S\lambda^+ S^{-1}U, \\ F^- &= S\lambda^- S^{-1}U. \end{aligned} \quad (11)$$

All the flux-splitting schemes prove to be dissipative, and thoughtful questions have been raised when applying them to the Navier–Stokes equations. For most viscous flux reconstruction, it must satisfy the discrete maximum principle and the linearity-preserving property in addition to the conservation law. In any event, the flux splitting schemes by van Leer [66] and Roe [67,68] are routinely and widely used to resolve shock waves in CFD applications. A collection of computed Mach number distributions across a normal shock at a free-stream value of 16 is presented in Fig. 4. These numerical results reflect the progress for shock-capturing technique that has been made over the years.

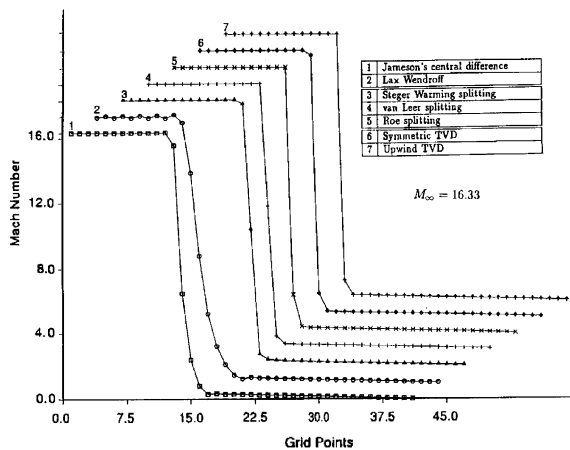


Fig. 4. Results of flux splitting schemes (courtesy of M. Aftosis).

In many ways, van Leer and Roe provided the impetuous in refining upwind schemes to evaluate convective fluxes using approximate Riemann solvers. Roe has pointed out that one could not expect to find a legitimate solution by solving differential equations in regions where the true solution is not differentiable. Therefore, the shock-capturing methods must be built on the integral rather than differential conservative laws. The numerical scheme also needs to incorporate the ideas drawn from the theory of characteristics. These resultant methods are robust and have been widely researched. A scholarly treatise by Roe [67] summarizing all characteristic methods was published in 1981. This paper probably is the article that has the highest literature citations in CFD and was selected for reprinting in 25th anniversary issue of Journal of Computational Physics. It is a text highly recommended to all. Both van Leer and Roe are respected as exceptional teachers and mentors to students in CFD.

On May 1, 1992, the CFD community endured a serious loss by the pre-mature passing away of Joseph L. Steger. There is no doubt that Steger was the most creative CFD pioneer. His outpouring of original ideas spans an extreme range from numerical algorithms for transonic flow, gas dynamics, overset grid, (he loved to call it Chimera), hyperbolic grid generator, and numerous challenging aerodynamic problems including the space shuttle in ascending flight. In addition, he was a caring and meticulous teacher to his students. Most of all, Steger was the standard bearer of the excellent and cherished CFD tradition—he shared his ideas unselfishly and enjoyed other's successes equally as his own.

#### 4.3. Unstructured grid technique

Applications of CFD for predicting aerodynamic performance extended to an ever-widening range to include automobile design, marine architecture, weather prediction, and internal combustion engines. The resources required in the pre-processing grid generation process for a complex configuration became a major portion of the entire simulation process. For example, the first F-16A aircraft simulation took 3 months for data processing on a CRAY-1 computer, another 3 months for validating and interpreting numerical results for engineering analysis, but required 11 months to generate the three-dimensional grids before computations could even start. The unstructured grid emerged in the late 1980s as a revolutionary change for CFD application. At the very beginning, only the Delaunay Scheme [69] was used for generating the two-dimensional triangular and three-dimensional tetrahedron mesh. A property of the Delaunay mesh requires that no other grid points be within a circumscribing sphere passing through the four points of a tetrahedron. From the analytic geometrical viewpoint, the pyramidal

control volume topology is natural to uniquely define the control surface. Since only three coplane points can be contained in a plane surface, the structured hexahedron grid must stipulate that the extra point resides in the same plane. Today, unstructured grid generation is highly developed and very efficient. Using the advancing front or Delaunay triangulation schemes, a mesh system around a complex aerodynamic shape can be obtained in days.

Morgan, Lohner, and others had long toiled in developing the finite-element algorithms for CFD [70]. However Jameson et al. [71], as well as, Stoufflet et al. [72] were among the first to apply the unstructured technique to complex aerodynamic configurations. In spite of the tremendous advantage of a shortened preprocessing time for numerical simulation, in its early stage of development the unstructured grid methodology suffered data structure redundancy and thus required excessive computer memory space and computing resources on vector processors than its structured grid counterpart. In addition, the immediately adjacent cells connectivity is often over determined for flux calculation on the control surface, so a least square or other approximation must be used in flux reconstruction to limit the spatial accuracy to second order. Although the quadrature reconstruction, in principle, can extend this method to higher order of accuracy [73], the misalignment of the control surface along the shock front is

detrimental to high-speed aerodynamic simulation. This shortcoming is reflected by multiple slip streams associated with high vorticity originating from misalignments. As a consequence, numerical results by an unstructured grid technique for the viscous–inviscid interaction without grid refinement can be inaccurate. This issue and the high-order method development for the unstructured grid method will remain as the mainstay for CFD research for some time to come.

As an illustration, an unstructured grid system at the joint of a diamond wing is presented in Fig. 5. The grid generation process was simple and straightforward. Although the wing intersection contains some concave surface segments and distinct surface topologic constructions, the grid generation has been accomplished without any difficulty. The numerical simulation was successfully followed shortly there after with only a minimum amount of effort to control the quality of the mesh system for the element skewness. In contrast to the hexahedron grid construction, the tetrahedron grid generation requires a minimum number of input data. Furthermore, the unstructured methodology has two unique and yet frequently overlooked attributes. First this grid system offers an advantage in solution-adaptive grid refinement, because it is intrinsic to the concept of an unstructured mesh. Secondly the neighbor-cell connectivity of an unstructured grid formulation enhances an exceptionally scalable, parallel computing

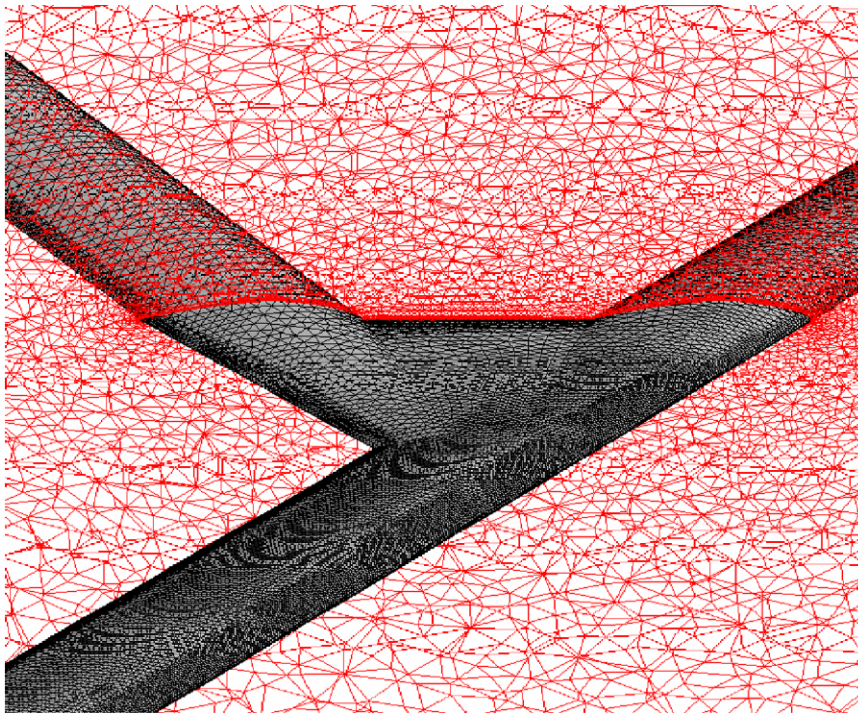


Fig. 5. Unstructured grid for wing joint (courtesy of C. Tyler).

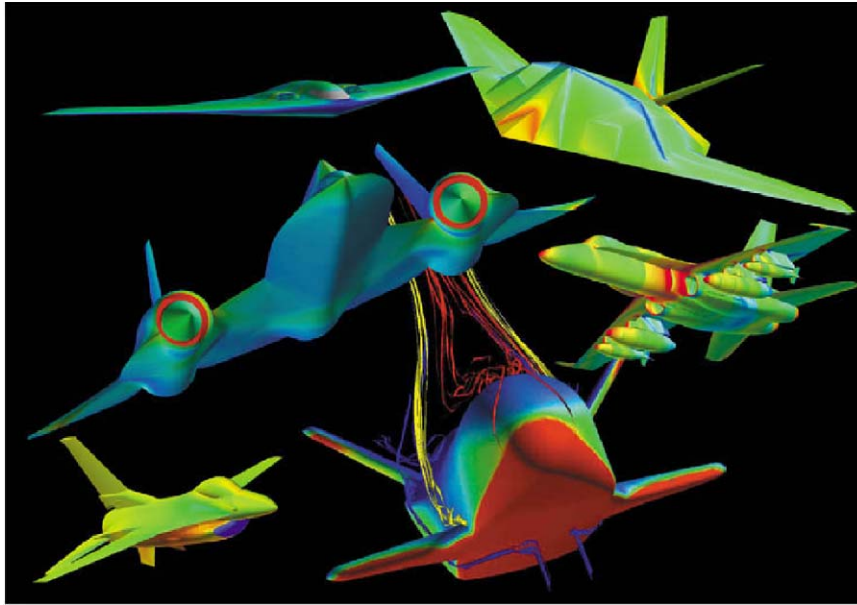


Fig. 6. CFD simulations of aerospace vehicle.

performance when this numerical procedure is ported to multi-computers using a domain decomposition strategy [74–76].

The massively parallel computing technology elevates the unstructured grid methodology to a higher level of performance. For processing a huge amount of data of complex physics or complicated aerodynamic shapes, a host of distributive (IBM SP, Cray T3D) and shared-distributive memory (Intel Origin 2000) computing systems was developed in the early 1990s. These massively parallel computing systems consisted of a large number of reduced instruction set computers (RISC) connected by a high-speed intercommunicating network. For large-scale computing simulations, the domain decomposition strategy is most efficient when using the message-passing paradigm [74,75]. The redundant data structure for the unstructured grid procedure is actually required for the domain decomposition approach. In addition, the load balancing for efficient parallel computing is nearly automatically achievable to make all unstructured grid procedures scalable. Astonishingly highly parallel numerical simulation efficiency and versatility of unstructured Navier–Stokes/Euler equations solvers has been demonstrated by the work of Strang et al. [76]. In Fig. 6, all numerical simulations for a wide range of aerospace vehicles were generated by a single computer program and provided practical aerodynamic performance data for engineering. A dream that one can evaluate the aerodynamic performance of any complete aircraft in two weeks has been realized over the past 30 years.

## 5. Recent progress

### 5.1. High-resolution algorithms

Despite these impressive accomplishments, our numerical algorithm efficiency has still fallen short of the theoretical limit for approximation in discrete space. According to the Nyquist frequency criterion, two discrete points per wavelength is the absolute minimum grid-point density needed to achieve a meaningful simulation of the physics [77]. A typical second-order method in use requires a grid density of 20–30 points per wavelength to maintain suitable engineering accuracy. Therefore, there is a realizable 1000-fold improvement of numerical efficiency for three-dimensional calculations. The more recent high-resolution algorithm research has made significant progress to bridge the gap between the spectral limit and conventional numerical procedures. The required computational efficiency for turbulence research and bringing CFD applications to interdisciplinary applications is paramount. This basic approach seeks algorithms that have a small stencil dimension and yet maintain a lower level of dispersive and dissipative error as compared to conventional numerical schemes.

Numerical resolution is naturally quantifiable by Fourier analysis in terms of normalized wave number. In applications, the grid-point density per wavelength provides the measuring metrics. All numerical schemes have a limited wave number range for accurate computations. However, this simple criterion becomes



insufficient when the computational domain consists of heterogeneous media with a wide range of characteristic impedances. The need to develop high-resolution schemes for extending the present simulation capability to higher frequency spectra is imperative.

Using the formal order of accuracy of truncation errors exclusively to select an algorithm for time-dependent simulation is an oversimplification [78–80]. The cutting edge effort by Tam and Weber [79] and Lele [80] are the most elucidated. According to Tam and Weber [79] and Lele [80], the desired feature of a numerical scheme may be derived from optimization in Fourier space rather by focusing on the lowest possible truncation error. In light of this line of reasoning, compact differencing and optimized finite differencing are viable methods by which to achieve high resolution. Both approaches seek algorithms that have a small stencil dimension and yet maintain a lower level of dispersive and dissipative error than the conventional numerical schemes. The basic idea of the compact difference approximation is not as radical as it sounds. Collatz has pointed out in the mid-1960s that the compact difference scheme is based on Hermite's generalization of the Taylor series [78].

The basic formulation of compact differencing is an implicit procedure for evaluating the derivatives of the dependent variables. The stencil structure for most compact-difference formulas is spatially central and requires additional derivative values at boundaries [80–82]. The spatially center scheme is inapplicable to the immediately adjacent mesh point at a boundary. An additional transitional numerical scheme from the boundary to the interior domain is required. The transitional boundary scheme not only requires transmitting data from the boundary but also preserving the stability and accuracy of interior domain for global resolution. This unique feature of compact-difference schemes also is one of the sources of spurious high-frequency oscillations. Furthermore, higher numerical resolution often exposes poorly imposed boundary conditions and poorly constructed meshes that are masked by numerical dissipation.

For the spatially central algorithms, both the boundary conditions as well as the mesh stretching have a profound effect on computational stability and accuracy, often leading to divergent results. A practical approach towards ensuring stability is using the mechanism of spatial filtering [81]. This effective remedy is derived from a procedure of modifying only the amplitude of Fourier components within a designated frequency spectrum. From experience in numerical analysis, the higher frequency components of solutions always become unstable first. Therefore, the numerical stability is enhanced by suppressing the amplitude of high-frequency Fourier components in the numerical solution. In fact, these components are already unsupported by the mesh system and are truly parasitic. The accomplishments in high-resolution algorithm research have developed several numerical procedures that approach the spectral-like performance for practical applications [77–82].

An unexpected benefit in using the spatial filter is revealed by its ability to eliminate the reflected wave in a finite computational domain. This unique feature is clearly demonstrated in Fig. 7. It was a fundamental challenge for time-dependent computational aeroacoustics and computational electromagnetics in a truncated computational domain. The most recent advancement made by Visbal and Gaitonde using the low-frequency bypass filter for suppressing time delay instability and enforcing the no-reflection boundary condition at the truncated computational far field are impressive [82].

## 5.2. DNS and LES

It is too well known that the Achilles's heel of CFD as a scientific discipline is the inadequate turbulence closure. It is also perfectly understandable in view of the fact that turbulence is still one of the outstanding problems in physics. A century has passed since the first turbulence experiment by Osborne Reynolds; at the present only the statistical theories of turbulence have generated reasonable scaling laws for turbulence [24,83,84]. There should not be any doubt that the

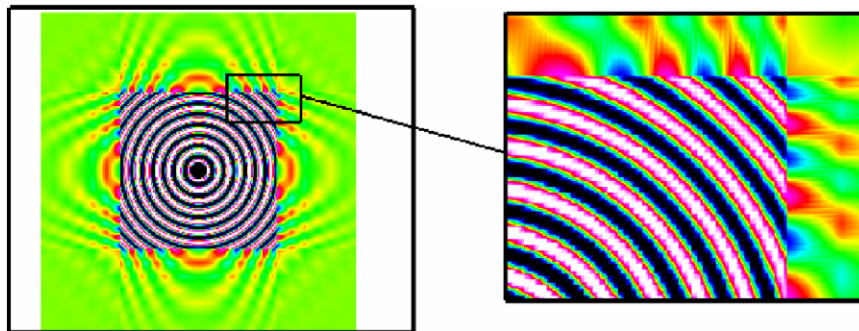


Fig. 7. No-reflection far field condition via spatial filter (courtesy of V. Visbal and D. Gaitonde).



correct physics is embedded in the time-dependent, three-dimensional Navier–Stokes equations. Unfortunately, turbulent flows have broadband spectra, and most numerical methods in CFD applications are inaccurate in resolving physics to the pertinent kinetic scales that carry significant energy. In addition, turbulence cannot be characterized in single space and time scales necessary to analyze the truncation error, like all other nonlinear problems, associated with a broad spectrum of scales. The discrete error of turbulent simulation may have to be analyzed in spectral space using the modified wave number [85]. The question remains as what is the most efficient numerical procedure required to resolve the formidable micro-scales and for the entire flow field. This critical research arena requires long-term vision, sustained support, and rigorous peer review.

The direct numerical simulation (DNS) of turbulence is the most straightforward approach to simulate turbulence. In principle, all the scales of motion can be resolved accurately and its application at the present time is limited by its cost. According to the Kolmogorov microscales, the ratio between the largest and smallest eddy of fluid motion is proportional to the three-quarter power of the characteristic Reynolds number,  $Re^{3/4}$  [24]. To resolve all scales of three-dimensional motion, the number of grid points required becomes astronomical and proportional to the value of  $Re^{9/4}$  [86]. The computing resource requirement even challenges the existing massively concurrent computers. For this reason, the DNS is used sparingly only for the laminar-turbulent transition, vorticity and energy production to acquire insight on the detailed spatial relations in kinematics and dynamics of turbulent eddies. The pioneering effort using direct numerical simulations by Fasel [52], and Rai and Moin [87] have offered a glimpse of promise. A more recent summary can be found in the work of Moin and Hahesh [83].

One of the most striking examples of using DNS to successfully simulate the laminar–turbulent transition was produced by Rist and Fasel [88]. In Fig. 8, the sequential numerical results of the fine-scale vortical structure in a boundary layer over a flat plate are presented from the rapid growth to breakdown processes. These numerical results actually show that the high shear layer indeed rides on top of the  $\Lambda$  vortex. This computed result fully substantiates early experimental observations to provide a new level of insight for the bifurcating phenomenon.

An intermediate approach to turbulent flow for complicated geometry and flow separation is the large eddy simulation (LES). The basic premise is that only the large eddies containing information about the geometry and dynamics of the flow have to be resolved, and the eddies of smaller scale have the universal structures according to Kolmogorov [24,84–86]. In spite of the elegance of this concept, realistically there is no

clear separation between the scales of large and small eddies. Nevertheless in LES, the contribution of the large energy-carrying structures to momentum and energy transfer is computed exactly. The systematic procedure in LES is built on the concept of a filter function that eliminates the small-scale fluctuations and retains only the smoothed large-scale structures.

$$\overline{U(r,t)} = \int U(r,t) f\left(\frac{r-\eta}{\Delta}\right) d\eta.$$

The resolvable large eddy motion is controlled by the filter width  $\Delta$  of the smoothing function. Meanwhile, the small-scale structures tend to depend mostly on viscosity and become somewhat universal. The effect of the smallest scales of turbulence is modeled [85, 86].

A primary function of the subgrid scale (SGS) model is to remove energy from the resolved scales to mimic the drain of the energy cascade [86]. Over the past decade the Smagorinsky model has demonstrated practical applications for flows over complicated geometries and complex flows containing multiple flow regimes [84–86]. However in applications, the coefficients in the model require tuning for different simulations like the turbulent closure models in the Reynolds averaged Navier–Stokes computations (RNS). The more recent advance in the dynamic SGS model by Germano et al. [89] are free from this limitation. The coefficients of the dynamic model are determined by the calculation procedure, based on the energy content of the smallest resolved scale rather than prior input.

In order to develop the crucial filter function and the SGS model, the mathematical structure of the Navier–Stokes equations have imposed constraints on the formulation. Ghosal has made several incisive observations [85]: First, the Navier–Stokes equations and all the basic laws of physics are Galilean invariant and the Navier–Stokes equations exhibit invariance under translation, rotation, reflection, and different scales. The spatial filter functions for LES shall preserve the symmetry under arbitrary Galilean transformation. Second, the requirement of a non-negative value of the turbulent kinetic energy or the so-called realizability of the SGS models needs to reinforce. In practice, the realizability condition is strict, validated only in the case of non-negative filters. Finally, the quadratic nonlinearity, such as  $u_i u_j$  is an inherent property of the Navier–Stokes equations. The power spectra of the numerical errors contain quadratic terms that can be invaluable to differentiate the physics and the numerical artifacts. Another interesting observation in accurate LES computation is that the practice of using a filter width significantly greater than the grid spacing, which highlights the basics of all numerical analyses in wave number space.

The experience in using LES has been enriched by applications to canonical problems, transitional flows,

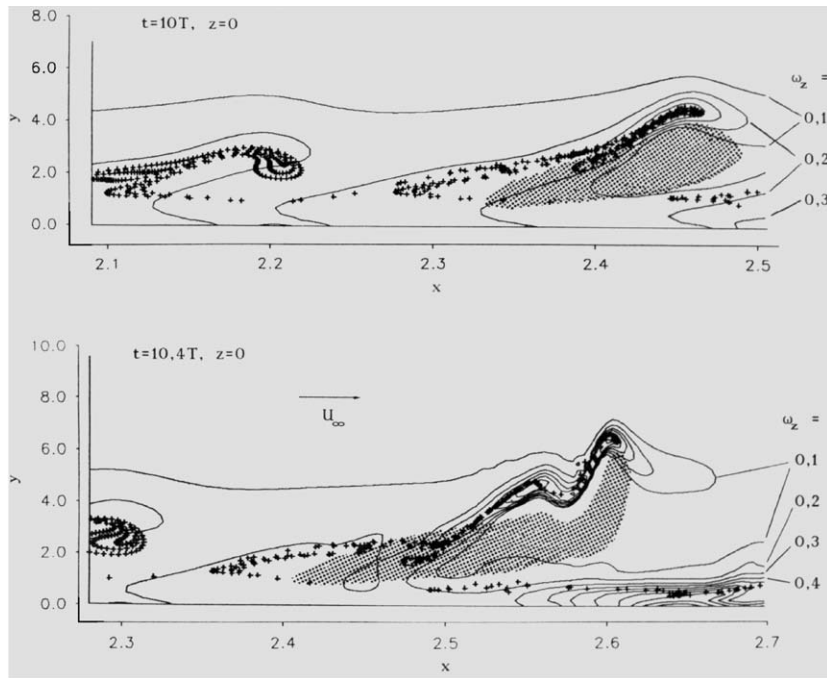


Fig. 8. Shear layer structures in a controlled transition (courtesy of H. Fasel).

unsteady or three-dimensional separated boundary layers, and flows over configuration with discontinuous surface segments. Recently the unstructured grid technique is further developed in LES research to have a novel feature that discretely conserves kinetic energy [90]. LES also shows great potential in breaking new ground for turbulent combustion and acoustics simulations. Lesieur and Metais [91] and Moin and Haehesh [83] have accomplished scholarly surveys to show encouraging progress and invaluable insights in LES and DNS research.

In summary, turbulence research is the vital area of fluid dynamics and the principal obstacle that prevents CFD to become a truly predictive tool and an internally consistent scientific discipline. The physics of turbulence is complex and always is a genuine three-dimensional, multiple-scale, nonlinear phenomenon. The challenge of turbulence is present in each and every engineering application, except perhaps in some very limited microfluidic environments. An unwavering and persisting support to this basic research arena is critical to sustain the future advancement of fluid dynamics and aerospace science.

## 6. Interdisciplinary computing simulation

CFD by definition is a multi-disciplinary endeavor, which requires the knowledge of fluid dynamics, applied

mathematics, and computing science. As a design tool, CFD can only provide the aerodynamic performance evaluation for a particular configuration. To analyze a complete aerospace vehicle's performance, the interaction between the structure and aerodynamic force, the thermodynamic dynamic properties of the high-temperature gas surrounding the flight vehicle and within the propulsive system, as well as the flight control and communication systems must be integrated into the iterative design process. All these requirements demand an in-depth physical understanding and modeling of these physics into a common frame with the aerodynamics. Therefore it is natural for CFD to expand into the interdisciplinary computational domain [92].

### 6.1. Aeroelasticity

As the application range expands, the level of engineering detail becomes more demanding. In transonic flight, the challenge to resolve the buffeting, limit-cycle oscillation, and flutter phenomena arises. The nonlinear interaction between aerodynamic forces and structure response can lead to catastrophic structure failure or become the limiter of air vehicle performance. The pioneering effort of Dowell in his study of panel flutter used linear aerodynamic models and was summarized in an exceptional review article of aeroelastic stability of plates and shells [93]. Some of these aeroelasticity problems can only be resolved by solving

the structural dynamic equations simultaneously with the Euler or Navier–Stokes equations. The early effort by Levy [48] and the more recent contribution by Obayashi and Guruswamy [94] is just the tip of the iceberg. Historically, the dynamic aeroelastic computations were performed using Euler or Navier–Stokes numerical procedures to solve flow field over 3D rigid bodies, then extended to include aeroelastic effects.

Today, the advance in nonlinear aeroelasticity progresses at a very rapid rate to address the long outstanding problems in structural response to aerodynamic forces and moments [95–99]. Nonlinear aerodynamic effects on transonic divergence, flutter, and limit-cycle oscillations were studied by the harmonic balance approach in the frequency domain, and extended into multiple structural degrees of freedom. The aerodynamic force in this analysis by Thomas et al. is calculated from the Euler equations [95]. In the same time frame, Gordnier and Visbal developed a more rigorous aerodynamic calculation procedure to solve the nonlinear panel flutter by coupling the three-dimensional Navier–Stokes equations and the von Karman plate equation [96]. In most numerical procedures, the aerodynamic and structural dynamic equations are solved in sequence or in a loosely coupled manner. A lagging error of numerical simulation was noticed. An innovative subiteration strategy was adopted to synchronize the solutions of aerodynamic motion and structural response. Their approach demonstrated that the elimination of a lagging error is important to study the temporal development of flutter as the computed results exhibit in Fig. 9.

The most recent developments for aeroelasticity simulation are focused on the introduction of the finite-element method for direct structural dynamics computations. Farhat and Lesoinne developed a variety of techniques for the coupling aerodynamic and structural dynamics computational methods [97]. They solved the coupled system of equations via a partition procedure in which a staggered algorithm is employed for the time discretized equation system. For a strongly coupled aerodynamic and structure phenomenon, Rungtong and Bathe implemented the finite-element method to both the fluid and structure formulations and solved fully coupled equations simultaneously [98]. Gordnier and Fifthen, on the other hand, coupled a Navier–Stokes solver with a nonlinear finite-element model for isotropic and orthotropic plates via a subiteration procedure [99]. Excellent agreement between the computed and theoretical results was obtained for all cases considered. In an effort to improve the computational efficiency of aeroelasticity, Dowell et al. have introduced the concept of reduced order aerodynamic models [100]. This area of research will lead to a wide range of aeroelasticity simulations for industrial applications.

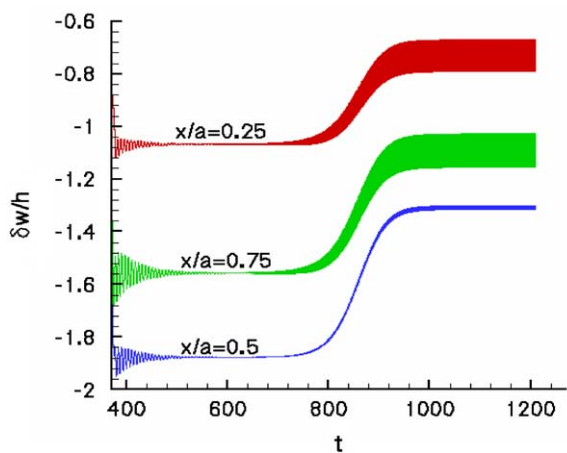


Fig. 9. Temporal development of flutter,  $M=0.5$  (courtesy of Gordnier and Visbal).

## 6.2. Aerothermodynamics

Hypersonic flow is one of the last few frontiers in aerodynamics because this flight region resides in the upper speed limit of flight, and more importantly, it is also the necessary passage for space access. This observation can be fully appreciated by the string of hypersonic vehicle programs worldwide such as the Star-H in France, Saenger/Horus in Germany, Hope in Japan, Hotol in United Kingdom, NASP in US, and Oryol (Raduga D-2) and Neva in the former USSR. The hypersonic flight vehicle must perform in an extreme high-temperature environment that brings in complex chemical kinetics issues beyond the combustion process for propulsive systems. For example, the air temperature around a reentry vehicle is around 12,000 K. At this temperature, the nitrogen is almost completely dissociated and is partially ionized. The problems of energy management and thermal protection require new material research and the complication of the rarefied gas effect also becomes pronounced in flight at extremely high altitude [101].

For high-speed CFD simulation in the hypersonic flow regime, the chemical kinetics must be considered [101,102]. Energy conversion from kinetic to thermal energy by the enveloping bow shock wave leads to a flow medium with nonequilibrium excited internal degrees of freedom. Fig. 10 yields a convincing illustration even at a moderate Mach number of 12. In this simulation, only the nonequilibrium dissociation of air is modeled and the chemical kinetics is solved simultaneously with the compressible Navier–Stokes equations [103]. It is clearly indicated that the standoff distance of the bow shock for the ogive-nosed blunt body is slightly reduced by the nonequilibrium gas effect, but the downstream flow field is profoundly altered. The simulated chemical kinetic

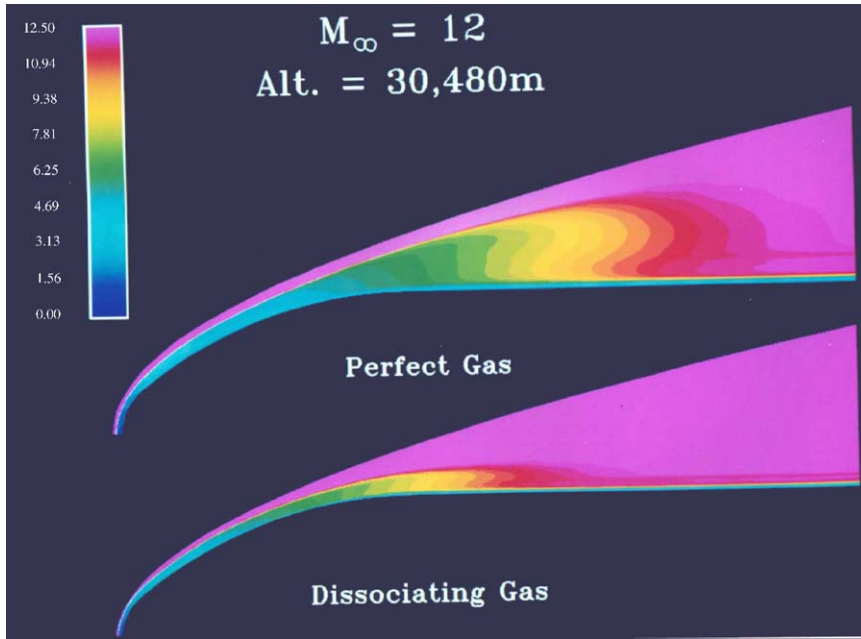


Fig. 10. Real gas effect on shock-layer structure.

relaxation within the shock layer also correctly describes the physics that is dominated by collision processes.

For interplanetary reentry simulation, the vehicle is required to perform in a high-temperature ionized air mixture. A total of 11 species of the air mixture must be considered:  $N_2$ ,  $O_2$ ,  $NO$ ,  $N$ ,  $O$ ,  $N_2^+$ ,  $O_2^+$ ,  $NO^+$ ,  $N^+$ ,  $O^+$ , and  $e^-$  [104]. The knowledge required for the high-temperature gas must be derived from statistical thermodynamics involving partition functions to model the rotational, vibrational, and electronic excitations. The macroscopic equilibrium properties of the individual chemical species can be obtained through a description of an assembly of microscopic particles using statistical mechanics. The fundamental quantity linking details of molecular structure to thermodynamic behavior is the partition function. The total internal energy of the gas mixture is derived from the factorization property of the partition functions [105],

$$Z = \sum_i g_i \exp\left\{-\frac{\varepsilon_i}{kT}\right\}, \quad (12)$$

$$Z = Z_{\text{trs}} Z_{\text{rot}} Z_{\text{vib}} Z_{\text{dis}} Z_{\text{ion}},$$

where  $\varepsilon_i$  denotes the energy level associated with the permissible quantum state of each particle, and  $g_i$  is the degeneracy of level  $i$ .

The complete physical-based simulation requires the description of finite-rate chemical reactions and quantum chemical physics for rotation, vibration, dissociation, and ionization excitations. For the finite-rate

chemical reaction calculation, there exists a huge base of experience in propulsion technology. The species concentration can be calculated from the law of mass action that is derived from the equations of reaction equilibrium for a general set of chemical reactions [105],

$$\sum_i v'_i \alpha_i = \sum_i v''_i \alpha_i, \quad (13)$$

where  $v'_\alpha$  and  $v''_\alpha$  are the stoichiometric coefficients of the chemical reaction and  $\alpha_i$  is the chemical species. For a system in chemical equilibrium, the partial pressure of the reacting species  $p_\alpha$  in the mixture must satisfy the law of mass action.

$$\Pi(p_\alpha/p^*)^{v'_\alpha - v''_\alpha} = \exp(-\Delta\varepsilon/kT). \quad (14)$$

In the above equation,  $\varepsilon$  is frequently referred to as the chemical potential and is a function of the partial pressure and temperature. The species concentrations of the chemically reacting system, including the dissociation and ionization can be calculated by the net reaction rate,

$$\left(\frac{d\alpha_i}{dt}\right)_j = (v''_{i,j} - v'_{i,j})K_{f,j}\Pi(\alpha_i)^{v'_{i,j}} + (v'_{i,j} - v''_{i,j})K_{b,j}\Pi(\alpha_i)^{v''_{i,j}}, \quad (15)$$

$$R_{f,i} = K_{f,i}(T)\Pi(\alpha_i)^{v'_{i,j}}, \quad R_{b,i} = K_{b,i}(T)\Pi(\alpha_i)^{v''_{i,j}}.$$

The so-called rate constants  $K_{f,i}$  and  $K_{b,i}$  are obtained from the data-fitting Arrhenius equation. The additional complication of physics from chemical reactions is far

beyond the species concentration computation. In a heterogeneous gas mixture, the diffusion phenomena also play a dominant role in gas dynamics [105]. The concerns are clearly linked to the uncertainty in determining transport properties of the gas mixture. Fortunately, the thermal, pressure, and forced diffusion mechanisms are negligible in most aerodynamic applications. The ordinary diffusion has traditionally and effectively been described by the similarity parameter, Lewis number.

In the nonequilibrium environment of hypersonic flights in the Earth's atmosphere, three different characteristic temperatures may exist. For engineering approximations, Park suggests that the translational-rotational temperature, the vibrational-electronic temperature, and the electronic thermal temperature shall be considered individually with some validation calculations [104]. For modeling the vibration and electronic excitations, there are approaches ranging from multi-temperature models, Landau-Taylor, to the Master equation [104–106]. The chemical and thermodynamic nonequilibrium simulation capability has also been successfully used for oxygen iodine laser development [101].

In hypersonic simulation computations, there is little doubt that the leaders of this field are Park [102], MacCormack and Candler [107], Gnoffo, and Moss [108,109]. Moss actually has sustained the rarefied gas dynamics research using the direct simulation Monte Carlo (DSMC) method. However, the pacing item for simulating hypersonic flow shall focus on the irreversible thermodynamic and nonequilibrium chemical kinetics phenomenon and the largely uncertain transport properties of the high-temperature gas. These shortfalls of fundamental knowledge in this area have hobbled the progress in hypersonic flow research since the 1960s. This scientific discipline is the cornerstone of statistical thermodynamics and yet has been overlooked. Engineering applications requiring validating database for high-temperature gas behavior in flight conditions are left wanting. This an area of research that is under funded and under explored.

### 6.3. Computational electromagnetics

James Clerk Maxwell established the fundamental equations of electromagnetics in 1873, and they were experimentally verified by Heinrich Hertz in 1888. The governing equations consist of the Faraday induction law, the generalized Ampere law, and Gauss laws for the electric and magnetic fields. The governing equations constitute a hyperbolic system and are the classic initial-value problem. Since the electric and the magnetic fields are closely interwoven, the Gauss laws usually are not included in the computing procedure but are satisfied by

the appropriately imposed initial conditions.

$$\begin{aligned}\frac{\partial \vec{B}}{\partial t} + \nabla \times \vec{E} &= 0, \\ \frac{\partial \vec{D}}{\partial t} - \nabla \times \vec{H} &= -\vec{J}, \\ \nabla \cdot \vec{B} &= 0, \\ \nabla \cdot \vec{D} &= 0.\end{aligned}\tag{16}$$

The boundary conditions for the governing equations are required on the interfaces of different media. Without exception, the tangential components of the electric field and the normal components of magnetic field are continuous across the boundary. The discontinuity of tangential component of magnetic intensity,  $H$  and the normal component of electric displacement  $D$  must be balanced by the surface current density  $J_s$  and the surface charge density  $\rho_s$ , respectively.

The computational capability developed in the CFD community has also effectively spun off into other simulation and modeling disciplines. However, the most effective sharing of knowledge is with the computational electromagnetics in the time domain (CEM) [110]. Traditionally, solutions of Maxwell equations were generated in the frequency domain by the Fourier transform or the separation of variables technique to isolate all electromagnetic computations at a given frequency. The resultant governing equation system is elliptic and linear in most applications; therefore, theoretical development was the mainstay of CEM in the frequency domain and it achieved a remarkable degree of sophistication.

Time-domain CEM was initiated in the IEEE community in 1966 by the pioneering effort of Yee using the middle point Leapfrog scheme to solve the time-dependent Maxwell equations [111]. His ingenuity is revealed by his insight of the interweaving nature of the electromagnetic field and his first use of staggered grids for treating electrical and magnetic fields separately but simultaneously. In the ensuing years, Umashankar, Taflove, Luebber, and others have developed this approach on the Cartesian frame to an impressive level of sophistication for electromagnetic wave scattering calculations [110–112].

In the late 1980s, the characteristic-based CFD technique in generalized curvilinear coordinates started to transfer to the CEM community [110]. In fact, Shankar [113] has led the way for this technical transition. The time-dependent Maxwell equations are classified as the hyperbolic partial differential system, and in nearly all practical applications the system of equations is linear. For the wave-motion-dominated simulations, the difficulties of propagating waves across media of different intrinsic impedances and performing calculations in a truncated computational domain are easily solved by the Riemann approximation. Therefore,



all characteristic-based methods developed in the CFD community are directly applicable to CEM [113–116]. In Fig. 11, the computed bistatic radar cross-sections of a perfectly electrical conducting sphere at three different frequencies are presented together with the Mie's series. Using the coordinate transformation technique, the radar cross sections of complete aircraft were obtained. The accuracy of numerical results was also verified by comparing with radar range data [110]. Equally important, these numerical procedures have been successfully ported onto massively parallel computers to expand the application frequency range of the CEM by orders of magnitude.

The influx of CFD techniques has enriched the tool set for electromagnetic research and solved many scattering problems from very large electrical shapes, radar range profiles, and transient phenomena associated with microwave horns, antennas, and micropatch antenna radiation [110, 113–116].

#### 6.4. Computational magneto-fluid dynamics

Computational magneto-fluid dynamics (CMD) is a natural extension of CFD application for hypersonic flows. In practical aerodynamic applications, the air requires a rather large amount of energy to achieve the ionized state by thermal collision process and energy transfer between internal degrees of freedom. For example, the ionization potentials for oxygen and nitrogen molecule are 13.6 and 14.6 eV, respectively, and the charged particles concentration for an effective magneto-aerodynamic interaction such as in the reentry

condition has the range from  $10^{12}$  to  $10^{16} \text{ cm}^{-3}$ . However, this condition is naturally occurring in most hypersonic flights. The strong compression of a bow shock wave converts nearly all kinetic energy to thermal energy. The air mixture bounded by the bow shock wave and the vehicle achieves highly excited internal energy modes. As the air temperature exceeds 5000 K, a fraction of the dissociating molecules will shed their electrons [117]. The ionized air mixture is then characterized by a finite value of electrical conductivity, which may exceed a value of 100 mho/m depending on the flight speed and altitude. The interaction of charged particles with an applied electromagnetic field generates the Lorentz force ( $J \times B$ ) and Joule heating ( $E \cdot J$ ) as additional mechanisms that influence aerodynamic performance. These observations were strongly supported by the pioneering effort by Bush, Meyer, Ziemer, and others [118,119].

Four decades ago, Resler and Sears recognized the tremendous application potential of the electromagnetic effect for enhanced aerodynamic performance [118]. Their vision introduces a new physical dimension into conventional aerodynamics to enrich the fluid dynamic behavior. The added coupling of velocity and temperature by plasma through Joule heating makes some impossible flow field manipulations realizable. One of the possible uses of the Lorentz force is to accelerate or decelerate plasma continuously without choking at subsonic or supersonic inlets. The flow orientation of plasma can also be altered by the intrinsic relationship of the Hall current and the helical trajectory in a magnetic field.

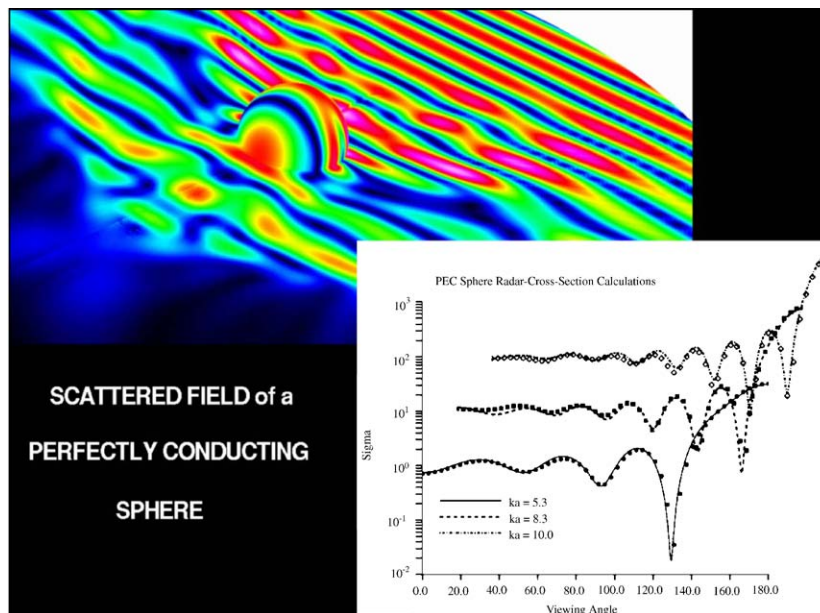


Fig. 11. Bistatic radar cross-section calculations at different frequencies.

The development of CMD for aerospace application really started a few years ago. Prior to the late 1990s, CMD were most concentrated on the problem in astrophysics and geophysics [119]. For studying these phenomena, the so-called ideal magneto-hydrodynamic (MHD) equation is adequate to describe all pertinent physics [120,121]. The MHD equations are nonconvex, thus, the wave structure is much more complicated than the Euler equations [120]. To simulate wave motion dominant phenomena, the characteristic-based or approximate Riemann algorithm in CFD, fits perfectly for solving the hyperbolic equation system [67,68]. Brio and Wu [120], and Powell et al. [121] were the first few to apply the upwind differencing schemes to solve the ideal MHD problems. Their numerical procedures were developed from the eigenvector structure of the non-strictly hyperbolic differential system. In essence, the governing equations consist of the approximate Maxwell equation for plasma physics and the Euler equations. In fact, both Brio and Wu adopted Roe's scheme and successfully simulated a MHD shock tube problem to show numerically for the first time the much more complex shock wave formation and wave propagation speed over that of aerodynamics [120]. Power et al. derived the flux splitting formulation for ideal MHD based on the four distinct wave speeds in plasma [121].

MacCormack has modified the Jacobian of the coefficient matrix for the flux splitting formulation of the magneto-fluid-dynamics (MFD) equations to preserve the homogenous of degree one property [122]. His effort allows the use of characteristic-based schemes for ideal MHD by Powell to solve the inviscid terms of the MFD equations [121]. Gaitonde has achieved the first ever and comprehensive three-dimensional MGD scramjet flow path simulation for propulsion enhancement [123]. In addition, MacCormack and Hoffmann et al. have led the interdisciplinary CMD development by including nonequilibrium chemical kinetics in their respective formulations [118,121].

MacCormack, Gaitonde, Hoffmann, and others have made impressive contributions to the maturation of CMD for aerospace application [119,122,123]. In CMD, the classic plasma assumptions of the electrically global neutrality and the negligible displacement current compared to the conducting current prevailed. In most aerospace applications, the magnetic Reynolds number,  $Re_{m} = \mu\sigma uL$  of the MFD field is also much less than unity; the induced magnetic field becomes negligible in contrast to the externally applied field. Therefore, the Faraday induction law can be decoupled from the governing equation system. Under this circumstance, the fluid medium is described as a single electrically conducting fluid with the usual dependent variables of fluid motion, and the Lorentz force and the Joule heating appear in the Navier–Stokes equations as

resource terms.

$$\begin{aligned} \frac{\partial \rho}{\partial t} + \nabla \cdot (\rho U) &= 0, \\ \frac{\partial \rho U}{\partial t} + \nabla \cdot (\rho U U + p\bar{I} - \bar{\tau}) - J \times B &= 0, \\ \frac{\partial \rho e}{\partial t} + \nabla \cdot [\rho e U + Q + U \cdot (p\bar{I} - \bar{\tau})] - E \cdot J &= 0, \\ \frac{\partial \rho e}{\partial t} + \nabla \cdot J &= 0. \end{aligned} \quad (17)$$

The last equation of the above governing system is adopted as a constraint and is known as the charge conservation equation, which is derived from the generalized Ampere law and Gauss laws for electric displacement. In solving the MFD equations, this equation usually is included to ensure a self-consistent electric field as a compatible condition. Meanwhile, Ohm's law is also required to relate the displacement current  $J$  and the electrical field  $E$ .

$$J = \bar{\sigma} \cdot [E + U \times B - \beta(J \times B) + \alpha(J \times B \times B)]. \quad (18)$$

In this formulation, the Hall effect and the ion slip are explicit contained in Ohm's law. For CMD computations, the distributions of electrical conductivity and the charged particles concentration are required. Again the description of transport properties for the electrically conducting medium presents a formidable challenge. In a high-temperature environment, the concentrations of a weakly ionized gas can be calculated by the chemical kinetics, such as the Saha equation [105,117]. However, the electrical conductivity of the gas is still unknown and frequently relies on plausible assumptions. For most recent magneto-aerodynamic actuator applications, the plasma generation is exclusively dependent on the secondary electron emission. In this mode of ionization, the thermal collision process does not apply. The freed electrons are obtained mainly from secondary emission caused by the bombardment of the cathode by positively charged ions, and this electro-dynamics phenomenon is controlled by the drift and diffusive motion of charged particles.

An international collaboration for glow discharge modeling by Surzhikov and Shang has taken place in 2002 [124,125]. They realized the vast majority of plasma generation processes in experiments are based on the gas discharge and launched a research effort based on the drift-diffusion model by Raizer [126]. For the three-component plasma model, the charged particles concentrations are computed by the continuity equations for the singly charged ions and electrons. The conservation of momentum equations for charged particles have replaced the approximate Ohm's law. In this formulation, the computed current density, electrical field intensity, and magnetic flux density are obtainable after satisfying the charge conservation law, and the external circuit equation,  $E = V_n + I_n R_n$ . Although additional

verification of the computing model is still required, this research result shows promise for practical application.

In order to expand physical dimensions for flow control and improved aerodynamic performance of aerospace vehicles, magneto-aerodynamic interaction is introduced into the hypersonic flows. In Fig. 12, a gas discharge from two electrodes parallel to the leading edge of a flat plate is implemented as a hypersonic flow control device [125]. The modified displacement thickness of the boundary layer by Joule heating is further amplified by viscous–inviscid interaction to produce a greater pressure plateau than the classic pressure interaction. The additional pressure increment by the magneto-aerodynamic actuator is equivalent to a one-degree deflection of the plate at a Mach number of 5.15. The total energy supply to this magneto-aerodynamic actuator for flow control is 60 W. The energy needed for practical flow control application can be scaled as 18.9 W/cm for the required electrode dimension. The computed pressure distributions have been verified by experimental observations [125].

To take this idea a step further, the magneto-aerodynamic interaction together with a nonlinear aerodynamic amplifier is equally applicable to create a virtual variable-geometry, hypersonic inlet for a combined cycle propulsive system. In principle, a series of segmented, glow discharge electrodes in a hypersonic inlet can generate a nearly isentropic compression that is impossible to achieve by a pure fluid dynamic mechanism alone [118].

In short, CMD has made impressive progress in the past few years. The predictive capability has advanced to a level of maturation for practical aerospace application [119,126,127]. The most efficient and accurate modeling

and simulation procedure is built on the low magnetic Reynolds assumption. The most recent research in magneto-aerodynamic includes fluid dynamics, electromagnetics, and chemical kinetics, which is the most complex governing equation system in computing science. A potential technologic breakthrough for improving aerodynamic performance is anticipated.

## 7. Outlook

In any human endeavor, the knowledge sharing among peers and passing from generation to generation is paramount to mature a scientific discipline to a new horizon. The education and training for CFD were strongly emphasized from day 1. There is a wonderful tradition in the aerospace industry of using workshop to bring new technology to the community. In the early 1970s, numerous CFD workshops were held either by government agencies or professional societies such as AIAA and ASME to compensate for the lack of textbooks. The workshop usually consisted of lectures and a few sample computer codes. In fact, it was the way one learned the basics in CFD at the very beginning. A lot of successful stories were originated from this type of training process.

Over the years, a series of excellent textbooks began to appear [9,10,128] and the learning process was also formalized. In most universities, CFD was offered in two to three consecutive classes; the syllabus roughly divided into the basics concepts of CFD, the classic algorithms, and numerical methods used. Professional societies have also sustained the seminar series and the self-study option. Most new generation CFD users educated under these more rigorous education programs tend to have a better grasp of the basics and benefited greatly from their formal training.

Now the most common practice for those who are proficient with workstations and PCs is to use Math Libraries or commercially available software packages. The computed results are displayed or analyzed with canned graphic software. However, the best practice shall still be derived from understanding the underlying physics and judiciously choosing a numerical procedure to achieve the best simulation. The computing error can be simply eliminated or alleviated by well-posed initial/boundary conditions and grid density refinement. However, the error incurred by using the inappropriate governing equation or initial/boundary conditions is uncorrectable. This required judgment can only be nurtured through rigorous education and training.

The future direction of CFD is easily determined from two overriding perspectives—faultless scientific foundation and practical application needs. It is too well known that the weakest link in CFD as a scientific discipline is

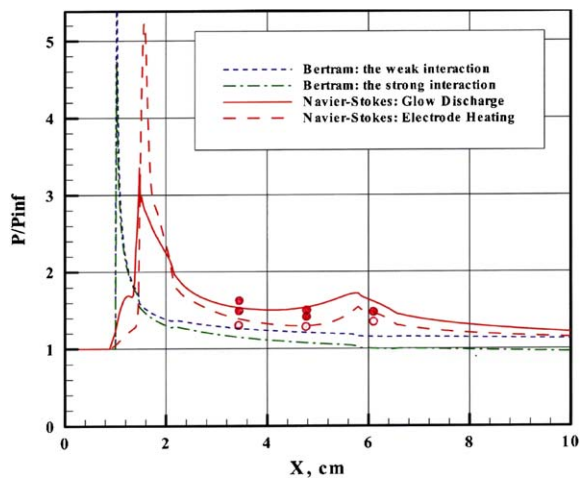


Fig. 12. Hypersonic magneto-aerodynamic interaction over flat plate.

the inadequate description of turbulence. This critical research arena requires long-term vision, sustained support, and rigorous peer review. The pioneering efforts using DNS and LES have opened research avenues for all to follow.

Modeling and simulation needs in aerospace engineering are clearly reflected by the unresolved and least understood problems in fluid dynamics, which are unsteady bifurcation and vortex interaction [92]. All these physical phenomena are nonlinear and have a strong element of time dependency associated with them. In the present context, bifurcation is defined as the transition between different dynamic states of fluid motion. The separated flow, laminar-turbulent transition, control surface buffeting and fluttering, lifting surface dynamic stall, inlet unstart, combustion instability, propulsive system surge, and rotating stall compressor all belong to this category. These phenomena are the aerodynamic performance pacing items, therefore they must be conquered with a consorted effort. As far as the vortex interaction is concerned Kuchemann has best described the importance of vortex dynamics in fluid dynamics—vortices are the sinews and muscles of fluid motion. Any future improvement in aircraft performance must rely on a better understanding and more accurate description of vortex interaction.

Equally important for future needs is system engineering. There is an urgent need to sustain the further development of interdisciplinary CFD capability. This ability to solve the show-stopping system issue and to weed out the unproductive ideas at the onset by interdisciplinary modeling and simulation tools will drastically shorten the design cycle and push CFD research for the unforeseeable future. In this sense CFD is not a mature technical discipline. However one should always bear in mind for future pursuit the two axioms from lessons learned; first, keep it simple but not simpler; it is truly an invaluable gift from Einstein. Second, research in CFD must return to basics to affect the widest applications; any basic research accomplishment will have a greatly enhanced value if it can be applied effectively.

## 8. Epilogue

Narrating a technical endeavor spanning nearly a century by an aerodynamicist and with a limited knowledge, numerous as well as significant contributions to CFD will be unintentionally overlooked either by author's limited exposure, personal bias, fading memory, or combination of these. Most importantly, the present effort only reflects a personal experience in a scientific discipline that is vast; please accept my sincere apology for any omission.

## Acknowledgements

The stimulating discussions with Prof. Robert W. MacCormack, Dr. Datta Gaitonde, Dr. Miguel Visbal, and helps in preparing this manuscript by my colleague, Prof. James Menart and Prof. David Johnston of Wright State University are sincerely appreciated.

## References

- [1] Richardson LF. The approximate arithmetical solution by finite differences of physical problems involving differential equations, with an application to the stresses in a masonry dam. *Phil Trans R Soc London, Series A* 1910;210:307–57.
- [2] Courant R, Friedrichs KO, Lewy H. Ueber die partiellen Differenzen-gleichungen der Math. Physik, *Math Ann* 1928;100:32–74.
- [3] Southwell RV. *Relaxation methods in engineering science*. London, UK: Oxford University Press; 1940.
- [4] von Neumann J, Richtmeyer RD. A method for the numerical calculation on the hydrodynamic shocks. *J Appl Phys* 1950;21:232–7.
- [5] Lax PD. Weak solution of nonlinear hyperbolic equations and their numerical computation. *Commun Pure Appl Math* 1954;7:159–63.
- [6] Godunov SK. Finite-difference method for numerical computational of discontinuous solution of the equations of fluid dynamics. *Mat Sb* 1959;47:271–306.
- [7] Riemann GFB. *Uber die Fortpflanzung Ebener Luftwellen von Endlicher Schwingungsweite*. *Abh Konigl Ges Wiss Gottingen* 1860;8:449.
- [8] Thom A. The flow past circular cylinder at low speeds. *Proc R Soc London, Series A* 1933;141:651–66.
- [9] Roache PJ. *Computational fluid dynamics*. Albuquerque, NM: Hermosa Publishers; 1976.
- [10] Tannehill JC, Anderson DA, Pletcher RH. *Computational fluid mechanics and heat transfer*, 2nd ed. Philadelphia, PA: Taylor & Francis; 1997.
- [11] Harlow FH. The particle-in-cell computing method for fluid dynamics. *Methods in computational physics*, vol.3. New York: Academic Press; 1964. p. 319–43.
- [12] Evans MW, Harlow FH, Meixner BD. Interaction of shock or rarefaction with a bubble. *Phys Fluids* 1962;5:651–6.
- [13] Amsden AA, Harlow FH. Numerical calculation of supersonic wake flow. *AIAA J* 1965;3:2081–6.
- [14] Butler TD. Numerical solutions of hypersonic sharp leading edge flows. *Phys Fluids* 1967;10:1205–15.
- [15] Lees L, Reeves BL. Supersonic separated and reattaching laminar Flows: I. General theory and application to adiabatic boundary-layer/shock-wave interactions. *AIAA J* 1964;2:1907–20.
- [16] Davis RT, Flugge-Lotz I. Second-order boundary effects in hypersonic flow past axisymmetric blunt bodies. *J Fluid Mech* 1964;20:593–623.
- [17] Stewartson K, Williams PG. Self-induced separation. *Proc R Soc London, Series A* 1969;312:181–206.

- [18] Burggraf OD, Rizzetta D, Werle MJ, Vatsa VN. Effect of Reynolds number on laminar separation of supersonic stream. *AIAA J* 1979;17(4):336–43.
- [19] Rakich JV. A method of characteristics for steady three-dimensional supersonic flow with application to inclined bodies of revolution. NASA TN D-5341; 1969.
- [20] Moretti G, Abbett M. A time-dependent computational method for blunt-body flows. *AIAA J* 1966;4(12): 2136–41.
- [21] Rubbert P. On the continuing evolution of CFD for airplane design. Conference text book, supercomputing, Japan-91. April 1991.
- [22] Navier M. Memoire sur les Lois du Mouvements des Fluides. *Mem Acad Sci Inst Fr* 1827;6:389.
- [23] Strikwerda JC. Initial boundary value problems for incompletely parabolic system. PhD dissertation, Stanford University, CA, 1976.
- [24] Friedlander SK, Topper L. Turbulence: classical papers on statistical theory. New York: Interscience Publisher; 1962.
- [25] Favre A. Equations des Gaz Turbulents Compressible. *J de Mec* 1965;4(3):361–90.
- [26] MacCormack RW. The effect of viscosity in hyper velocity impact cratering. AIAA paper 69-354; 1969.
- [27] Baldwin BS, MacCormack RW. Numerical solution of the interaction of a strong shock wave with a hypersonic turbulent boundary layer. AIAA paper 74-558; 1974.
- [28] Hung CM, MacCormack RW. Numerical solutions of supersonic and hypersonic laminar flows over two-dimensional compression corner, AIAA 75-2; 1975.
- [29] Horstman CC, Kussoy MI, Coakley TJ, Rubesin MN, Marvin JG. Shock-wave induced turbulent boundary-layer separation at hypersonic speeds. AIAA 75-4; 1975.
- [30] Shang JS, Hankey WL. Numerical solution of the Navier–Stokes equations for supersonic turbulent flow over a compression ramp. AIAA 75-3; 1975. AIAA J 1975;13(10):1368–74.
- [31] Knight DD. Numerical simulation of realistic high-speed inlets using the Navier–Stokes equations. AIAA J 1977;15:1583–9.
- [32] Dolling DS. Fifty years of shock/boundary interaction: what next. AIAA J 2001;39:1517–31.
- [33] Shang JS, Hankey WL. Numerical solution of the compressible Navier–Stokes equations for a three-dimensional corner. AIAA 77-169, 1979; AIAA J 1977;15: 1575–82.
- [34] Murman EM, Cole JD. Calculation of plane steady transonic flows. AIAA J 1971;9:114–21.
- [35] Jameson A. Iterative solution of transonic flows over airfoils and wings including flows at mach 1. *Commun Pure Appl Math* 1974;17:283–309.
- [36] Thompson JF, Thames FC, Mastin CW. Automatic numerical generation of body-fitted curvilinear coordinate system for field containing any number of arbitrary two-dimensional bodies. *J Comput Phys* 1974;15: 299–319.
- [37] Steger JL, Sorenson RL. Use of hyperbolic partial differential equations to generate body fitted coordinates, numerical grid generation techniques. NASA Conference Pub. 2166; 1980. p. 463–78.
- [38] Eiseman PK, Smith RE. Mesh Generation using algebraic techniques, numerical grid generation techniques. NASA Conference Pub. 2166; 1980. p. 73–120.
- [39] Thomas PD, Lombard CK. The geometric conservation law—a link between finite-difference and finite-volume methods of flow computation on moving grids. AIAA 78-1208; 1978.
- [40] Peaceman DW, Rachford HH. The numerical solution of parabolic and elliptic differential equations. *J Soc Ind Appl Math* 1955;3:28–41.
- [41] Douglas J, Gunn J. A general formulation of alternating direction methods, I, parabolic and hyperbolic problems. *Numer Math* 1964;6:428–53.
- [42] Briley WR. A numerical study of laminar separation bubbles using the Navier–Stokes equations. *J Fluid Mech* 1971;47:713–36.
- [43] Briley WR, McDonald H. Solution of the three-dimensional compressible Navier–Stokes equations by an implicit technique. Lecture notes in Physics, vol. 35. New York: Springer; 1974. p. 105–10.
- [44] Beam RM, Warming RF. An implicit factored scheme for the compressible Navier–Stokes Navier Stokes equations. AIAA J 1978;16:393–401.
- [45] Pulliam TH, Steger JL. Implicit finite difference simulation of three-dimensional compressible flow. AIAA J 1980;18(2):159–67.
- [46] Brandt A. Multi-level adaptive technique (MALT) for fast numerical solution to boundary value problem. Lecture notes in physics, vol. 18. Berlin: Springer; 1973. p. 82–9.
- [47] Rudman S, Rubin SG. Hypersonic viscous flow over slender bodies with sharp leading edges. AIAA J 1968; 6(X):1883–9.
- [48] Levy LL. Experimental and computational steady and unsteady transonic flows about a thick airfoil. AIAA J 1978;16(6):564–72.
- [49] Steger JL, Bailey HE. Calculation of transonic aileron buzz. AIAA J 1980;18(3):249–55.
- [50] Tassa Y, Sankar NL. Dynamic stall of an oscillating airfoil in turbulent flow using time dependent Navier–Stokes equations. Unsteady turbulent shear flows. New York: Springer; 1981. p. 185–96.
- [51] Drummer PJ, Weidner EH. Numerical study of a scramjet engine flow field. AIAA J 1982;20(9):1182–7.
- [52] Fasel H. Investigation of the instability of boundary layers by a finite-difference model of the Navier–Stokes equations. *J Fluid Mech* 1976;72(2):355–83.
- [53] Helliwell WS, Dickinson RP, Lubard SC. Viscous flow over arbitrary geometries at high angle of attack. AIAA J 1981;19(2):191–7.
- [54] Shang JS, Scherr SJ. Navier–Stokes solution for a complete reentry configuration. AIAA 85-1509; *J Aircraft* 1986;23(12):881–8.
- [55] MacCormack RW, Paullay AJ. Computational efficiency achieved by time splitting of finite difference operators. AIAA 72-154; 1972.
- [56] Rizzi A, Inouye M. Time-splitting finite-volume method for three-dimensional blunt-body flow. AIAA J 1973; 11(11):1478–85.
- [57] Thomas JL, Walters RW. Upwind relaxation algorithms for the Navier–Stokes equations. AIAA 85-1501; 1985.



- [58] MacCormack RW. Current status of numerical solutions of the Navier–Stokes equations. AIAA 85-0032; 1985.
- [59] van Leer B. On the relation between the upwind differencing schemes of Godunov, Enquist–Osher, and Roe. *SIAM J Sci Stat Comput* 1984;5:1–20.
- [60] Harten A. High-resolution schemes for hyperbolic conservation laws. *J Comput Phys* 1983;49:375–85.
- [61] Osher S, Chakravarthy SR. Upwind schemes and boundary conditions with applications to Euler equations in general coordinates. *J Comput Phys* 1983;50:447–81.
- [62] Busemann A. Drucke auf Kegelformige Spitzen bei Bewegung mit Überschallgeschwindigkeit, *Z. Angew Math. Mech.* Vol. 9, 1929, p. 496.
- [63] Ferri A. Elements of aerodynamics of supersonic flows. New York: Macmillan; 1949.
- [64] Boris J, Book D. Flux-corrected transport: I SHASTA, a fluid transport algorithm that worked. *J Comput Phys* 1973;11:38–69.
- [65] Steger JL, Warming RF. Flux vector splitting of the inviscid gas dynamics equations with application to finite difference methods. *J Comput Phys* 1981;40:263–93 NASA TM D-78605; 1979.
- [66] van Leer B. Flux vector splitting for the Euler equations. Lecture notes in physics, vol. 170. New York: Springer; 1982. p. 507–12.
- [67] Roe PL. Approximate Riemann solvers, parameter vectors and difference schemes. *J Comput Phys* 1981; 43:357–72.
- [68] Roe PL. Characteristic-based schemes for Euler equations. *Annu Rev Fluid Mech* 1986;8:337–65.
- [69] Delaunay B. Sur la Sphere Vide. *Bull Acad Sci, USSR, VII, Class Sci Mat Nat* 1934; 793–800.
- [70] Lohner R, Morgan K, Zienkiewicz T. An adaptive finite element procedure for compressible high speed flows. *Comput Methods Appl Mech Eng* 1985;51:441–65.
- [71] Jameson A, Baker TJ, Weatherill NP. Calculation of inviscid transonic flow over a complete aircraft. AIAA 86-0103; January 1986.
- [72] Stoufflet B, Periaux J, Fezoui F, Dervieux A. Numerical simulation of 3-D hypersonic Euler flows around space vehicles using adaptive finite elements. AIAA 87-0560; January 1987.
- [73] Barth TJ, Frederickson PO. High-order solution of the Euler equations on unstructured grids using quadratic reconstruction. AIAA 90-0013; January 1990.
- [74] Simmon HD. Partitioning of unstructured problems for parallel processing. *Comput Syst Eng* 1991;2:135–48.
- [75] Shang JS, Wagner M, Pan Y, Blake DC. Strategies for time domain CEM computations on multicomputers. *IEEE Comput Sci Eng* 2000;2(1):10–21.
- [76] Strang WZ, Tomaro RF, Grismer MJ. The defining methods of cobalt: a parallel, implicit, unstructured Euler/Navier–Stokes flow solver. AIAA 99-0786; January 1999.
- [77] Gottlieb D, Orsag S. Numerical analysis of spectral methods. Philadelphia: SIAM; 1997.
- [78] Collatz L. The numerical treatment of differential equations. New York: Springer, 1966. p. 538.
- [79] Tam CKW, Weber JC. Dispersion-relation-preserving finite difference schemes for computational acoustics. *J Comput Phys* 1977;24:10–22.
- [80] Lele SK. Compact finite difference schemes with spectral-like resolution. *J Comput Phys* 1992;103:16–42.
- [81] Gaitonde DV, Shang JS, Young JL. Practical aspects of higher-order numerical schemes for wave propagation phenomena. *Int J Numer Methods Eng* 1999;45:1849–69.
- [82] Visbal MR, Gaitonde DV. On the use of higher order finite difference schemes on curvilinear and deforming mesh. *J Comput Phys* 2002;181:155–85.
- [83] Moin P, Haresh K. Direct numerical simulation: a tool in turbulent research. *Annu Rev Fluid Mech* 1998;30: 539–78.
- [84] Piomelli U, Balaras E. Wall-layer models for large-eddy simulations. *Annu Rev Fluid Mech* 2002;34:349–74.
- [85] Ghosal S. Mathematical and physical constraints on LES. AIAA 98-2803, Albuquerque, NM, June 1998.
- [86] Piomelli U. Large-eddy simulation: achievements and challenges. *Prog Aerospace Sci* 1999;35:335–62.
- [87] Rai MM, Moin P. Direct numerical simulation of turbulent flow using finite-difference schemes. *J Comput Phys* 1991;96:15–53.
- [88] Rist U, Fasel H. Direct numerical simulation of controlled transition in a flat-plate boundary layer. *J Fluid Mech* 1995;298:211–48.
- [89] Germano M, Piomelli U, Moin P, Cabot WH. A dynamic subgrid-scale eddy viscosity model. *Phys Fluids* 1991; A3:1760–5.
- [90] Moin P. Advances in large eddy simulation methodology for complex flows. *Int J Heat Fluid Flow* 2002;23:710–20.
- [91] Lesieur M, Metais O. New trends in large-eddy simulations of turbulence. *Annu Rev Fluid Mech* 1996;28: 45–82.
- [92] Shang JS. Assessment of technology for aircraft development. *J Aircraft* 1995;32(3):611–7.
- [93] Dowell EH. Panel flutter: a review of the aeroelastic stability of plates and shells. *AIAA J* 1970;8:385–99.
- [94] Obayashi S, Guruswamy G. Unsteady shock-vortex interaction on a flexible delta wing. *J Aircraft* 1992; 26(5):790–8.
- [95] Thomas JP, Dowell EH, Hall KC. Nonlinear inviscid aerodynamic effects on transonic divergence, flutter, and limit-cycle oscillations. *AIAA J* 2002;49:638–46.
- [96] Gordnier RE, Visbal MR. Development of a three-dimensional viscous aeroelastic solver for nonlinear panel flutter. *J Fluid Struct* 2002;16:497–727.
- [97] Farhat C, Lesoinne M. Mixed explicit/implicit time integration of couple aeroelastic problems: three-field formulation geometric conservation and distributed solution. *Int J Numer Meth Fluids* 2001;21:807–35.
- [98] Rugonyi S, Bathe KJ. On finite element analysis of fluid flows fully coupled with structural interaction. *Comput Model Eng Sci* 2001;2:195–212.
- [99] Gordnier RE, Fithen R. Coupling of a nonlinear finite element structural method with a Navier–Stokes solver. *Comput Struct* 2003;81:75–89.
- [100] Dowell EH, Thomas JP, Hall KC. Transonic limit cycle oscillation analysis using reduced order aerodynamic models. AIAA 2001-1212; April 2001.
- [101] Shang JS. Numerical simulation of hypersonic flows. In: Murthy T, editor. Computational methods in hypersonic aerodynamics. Boston: Kluwer Academic Publisher; 1991. p. 81–114.

- [102] Park C. Non-equilibrium hypersonic aero-thermodynamics. New York: Wiley; 1990.
- [103] Josyula E, Shang JS. Numerical study of hypersonic dissociated air past blunt bodies. *AIAA J* 1991;29:704–11.
- [104] Park C. A review of reaction rates in high temperature air. AIAA 89-1740; Buffalo, NY, 1989
- [105] Clarke JF, McChesney M. The dynamics of real gas. Washington: Butterworths; 1964.
- [106] Josyula E, Bailey WF. Vibration-dissociation coupling using master equations in nonequilibrium hypersonic blunt-body flow. *J Thermophys Heat Transfer* 2001;15:157–67.
- [107] Candler GV, MacCormack RW. The Computation of hypersonic ionized flows in chemical and thermal nonequilibrium. *J Thermophys Heat Transfer* 1991;5(3):266–73.
- [108] Gnoffo PA, Weilmuenster KJ, Hamilton HH, Olynick DR, Venkatapathy E. Computational aerothermodynamic design issues for hypersonic vehicles. *J Spacecraft Rockets* 1999;36:21–43.
- [109] Moss JN. DSMC computations for regions of shock/shock and shock/boundary layer interaction. AIAA 2001-1027; Reno, NV, 2001.
- [110] Shang JS. Shared knowledge in computational fluid dynamics, electromagnetics, and magneto-aerodynamics. *Prog Aerospace Sci* 2002;38(6–7):449–67.
- [111] Yee KS. Numerical solution of initial boundary value problems involving Maxwell equations in isotropic media. *IEEE Trans Antennas Propag* 1966;AP-14:302–6.
- [112] Tafflove A. Computational electromagnetics, the finite-difference time-domain method. Boston: Artech House Inc.; 1995.
- [113] Shankar V, Hall WF, Mohammadian AH. A time-domain differential solver for electromagnetic scattering problems. *Proc. IEEE* 1989;77(5):709.
- [114] Shang JS. Characteristic based methods for the time-domain Maxwell equations. AIAA 91-0606; Reno, NV, 1991.
- [115] Shang JS, Gaitonde D. Characteristic-based, time-dependent Maxwell equation solver on a general curvilinear frame. *AIAA J* 1995;33(3):491–8.
- [116] Shang JS. Characteristic-based algorithms for solving the Maxwell equations in the time domain. *Antennas Propag* 1995;37(3):15–25.
- [117] Zel'dovich YaB, Raizer YuP. Physics of shock waves and high-temperature hydrodynamic phenomena. Minola, NY: Dover Publications Inc.; 2002.
- [118] Resler EL, Sears WR. The prospects for magneto-aerodynamics. *J. Aeronaut Sci* 1958;25:235–245, 258.
- [119] Shang JS. Recent research in magneto-aerodynamics. *Prog Aerospace Sci* 2001;37:1–20.
- [120] Brio M, Wu CC. An upwind differencing scheme for the equations of ideal magnetohydrodynamics. *J Comput Phys* 1988;75:400–22.
- [121] Powell KG, Roe PL, Myong RS, Gombosi T, Aee DD. An upwind scheme for magnetohydrodynamics. AIAA95-1704-CP; 1995. p. 661–71.
- [122] MacCormack RF. An upwind conservation form method for the ideal magnetohydrodynamics equations. AIAA 99-3609; June 1999.
- [123] Gaitonde DV. Numerical exploration of 3-D turbulent scramjet flowpath with MGD control. AIAA-2003-0172; January 2003.
- [124] Surzhikov ST, Shang JS. Glow discharge in magnetic field. 41st Aerospace Science Meeting. AIAA 2003-1054; Reno, NV, 2003.
- [125] Shang JS, Surzhikov ST. Magneto-fluid-dynamics interaction for hypersonic flow control. AIAA 2004-0508; Reno, NV, 2004.
- [126] Raizer YuP, Surzhikov ST. Two-dimensional structure of the normal glow discharge and the role of diffusion in forming of cathode and anode current spots. *High Temperature* 1988;26(3):169–77.
- [127] Shang JS. Historical perspective of magneto-fluid-dynamics. Introduction to magneto-fluid-dynamics for aerospace applications, Lecture Series 2004-01. Rhode-ST-Genese, Belgium: von Karman Institute for Fluid Dynamics; October 2003.
- [128] Hirsch Ch. Numerical computation of internal and external flows, vols. I & II. Chichester: Wiley; 1990.